U.PORTO

MESTRADO

ONCOLOGIA

Genetic characterization of upper urinary tract urothelial carcinoma

Ana Carolina Cunha Dias

M

2021

U.PORTO

Carolina Dias. Genetic characterization of upper urinary tract urothelial carcinoma

M.ICBAS **2021**

Genetic characterization of upper urinary tract urothelial carcinoma

Ana Carolina Dias

INSTITUTO DE CIÊNCIAS BIOMÉDICAS ABEL SALAZAR

Ana Carolina Cunha Dias

Genetic characterization of upper urinary tract urothelial carcinoma

Dissertação de Candidatura ao grau de Mestre em Oncologia – Especialização em Oncologia Laboratorial, submetida ao Instituto de Ciências Biomédicas Abel Salazar da Universidade do Porto.

Orientador – Professora Doutora Ana Paula Soares Dias Ferreira
Categoria – Professora auxiliar.
Afiliação – Faculdade de Medicina da Universidade do Porto e coordenadora do grupo *Cancer Signalling and Metabolism* do Instituto de Investigação e Inovação em Saúde do Porto/ Instituto de Patologia e Imunologia Molecular da Universidade do Porto.
Co-orientador – Doutor Rui Pedro Monteiro Batista
Categoria – Colaborador
Afiliação – Instituto de Patologia e Imunologia Molecular da Universidade do Porto (Ipatimup), Instituto de Investigação e Inovação em Saúde (i3S)

“Maybe I made a mistake yesterday, but yesterday’s me is still me. I am who I am today, with all my faults. Tomorrow I might be a tiny bit wiser, and that’s me, too.”

— Kim Namjoon

Agradecimentos

A concretização desta etapa deve-se, principalmente, à ajuda e ao apoio incondicional de diversas pessoas, às quais devo a minha maior gratidão.

Gostaria de agradecer primeiramente à minha orientadora, Professora Doutora Paula Soares. Muito obrigada por me orientar, não só neste último ano, mas desde que comecei o meu percurso no laboratório. Já se passaram dois anos e não poderia deixar de agradecer a oportunidade que foi aprender com a Professora.

Gostaria de agradecer também à Dra. Sara Meireles. Sem o seu auxílio e disponibilidade, esta tese não seria possível.

A todos os membros do “Cancer Signalling & Metabolism”, obrigada por todo o apoio e amizade constantes. Serei sempre grata.

Acima de tudo, agradeço a um grupinho especial. Aos que me souberam ouvir, apoiar, ajudar. Sofia, Elisa, Tiago, Ana. Este ano foi difícil, mas a vossa companhia deu-me forças para superar tudo. Um abracinho muito grande para cada um de vocês.

Aos meus amigos: muito obrigada por se manterem sempre ao meu lado e puder contar sempre convosco. Um brinde a vocês e a tudo o que já vivemos.

Deixo o agradecimento mais especial à minha família. Aos que mais me incentivam, aos que mais me apoiam, um beijinho grande e um abraço parte costelas.

Index of Contents

Index of Figures

Index of Tables

Index of Annexes

Abbreviations

AAN – Aristolochic Acid Nephropathy

BEN – Balkan Endemic Nephropathy

CK – Cytokeratin

CHUSJ – Centro Hospitalar Universitário de São João

Cis/Tis – Carcinoma *in situ*/Tumor *in situ*

CTU – Computed tomography urography

DAB – Diaminobenzidine chromogen

DNA – Deoxyribonucleic acid

ERK – Extracellular-signal-regulated kinase

ETS – E-twenty-six

FDA – Food and Drug Administration

FFPE – Formalin-Fixed, Paraffin-Embedded

FOXA1 – Forkhead Box A1

FGFR – Fibroblast growth factor receptor

FGFs – Fibroblast growth factors

GAPs – GTPase-activating proteins

GATA3 – GATA-binding protein 3

GDP – Guanosine-5'-diphosphate

GEFs – Guanine nucleotide exchange factors

GTP – Guanosine-5'-triphosphate

HG – High-grade carcinomas

HNPCC – Hereditary Non-Polyposis Colorectal Carcinoma

HRP – Horseradish peroxidase

h*TERT* – Human telomerase reverse transcriptase

ISUP – International Society of Urological Pathology

LG – Low-grade carcinomas

LN – Lymph node

LNA – Locked Nucleic Acid

LND – Lymph node dissection

LNM – Lymph node metastases

LRNU – Laparoscopic Radical nephroureterectomy

MAPK - Mitogen-activated protein kinase pathway

MEK - Mitogen-activated protein kinase

MIC – Muscle invasive carcinoma

MR – Magnetic resonance

Mut – Mutant

NMIBC – Non-muscle invasive carcinoma

NTC – Non-template control

PCR – Polymerase chain reaction

PD-1 – Programmed cell death protein-1

PDL-1 – programmed cell death ligand-1

PI3K – Phosphoinositide 3-kinase

PUNLMP – Papillary urothelial neoplasm of low malignant potential

qPCR – Quantitative PCR

RAF1 – Raf-1 proto-oncogene

RAS – Rat sarcoma viral oncogenes homologue

RB1 – Retinoblastoma 1

RNU – Radical nephroureterectomy

SEER – Surveillance, Epidemiology, and End Results Program

TCGA – The Cancer Genome Atlas

TKR – Tyrosine kinase receptor

UC – Urothelial carcinoma

UCB – Urothelial carcinoma of the bladder

UTUC – Upper tract urothelial carcinoma

WHO – World Health Organization

Abstract

The standard diagnostic methods and treatment options for upper tract urothelial carcinoma (UTUC) are derived from bladder cancer due to knowledge gaps regarding disease management. Patients are often submitted to invasive and uncomfortable procedures during the follow-up period. Thus, non-invasive alternatives are urgent, but still an unmet need. Genomic studies and stronger molecular evidence are required to identify molecular subgroups with distinct pathways of pathogenesis that can have prognostic and therapeutic implications in UTUC.

The main aim of this study is to characterize the genetics of UTUC and enlighten the potential use of genetic biomarkers in disease management and prognosis. In that regard, we planned to establish the status of FGFR3, TERTp, and RAS genes in a selected series of UTUC patients and to establish correlations between clinicopathological characteristics and molecular data. Additionally, we planned to evaluate the expression of immunohistochemical markers (CK5/6 and CK20) to differentiate the background of clinically relevant UTUC molecular subtypes.

A cohort study of patients with a confirmed diagnosis of UTUC was selected for molecular characterization. FFPE tissue blocks were sectioned for gene expression analysis and immunohistochemistry. The mutational tumor profile was assessed for FGFR3 and TERTp genes by real-time quantitative Polymerase Chain Reaction (qPCR), while RAS genes (HRAS, KRAS, and NRAS) were assessed by standard PCR and sequencing methods. The immunohistochemistry panel was comprised of basal (CK5/6) and luminal (CK20) markers.

Univariate and multivariate analyses were performed to estimate correlations between clinicopathological and molecular alterations of tumor tissue samples using the latest version of SPSS.

In 141 UTUC samples, 106 (75,2%) were mutated for at least one of the studied genes. The following mutation frequencies were found in this cohort: 55.5% for *FGFR3*, 54.2% for *TERT*p, 6.4% for *KRAS*, 2.1% for *HRAS*, and 0.7% for *NRAS*. In the present study, we observed that venous invasion was the only predictive factor of distant metastasis and that *FGFR3* mutations were statistically associated with the absence of lymphatic and venous invasion, denoting their effect as markers of good prognosis. *NRAS* mutations were associated with younger age, although only one mutation was identified. No associations were found between clinicopathological data and other *RAS* or *TERT*p alterations. Concomitant alterations between FGFR3 and TERTp genes were statistically significant, as expected.

In most tumors, we observed an aberrant expression pattern of CK5/6 and CK20, extended beyond the basal/intermediate and luminal layers, respectively. Comparing histological grades, we observed that all cases with negative expression (0) for CK5/6 and CK20 and all cases with the maximum score given were high-grade tumors. Those results are still preliminary and complementary studies (e.g.GATA3 expression) will be necessary to fully characterize the molecular subtypes in UTUC and its correlation with molecular and prognostic data.

Key-words: Immunohistochemical markers | Molecular alterations | Mutational profile | Upper urinary tract urothelial carcinoma

Resumo

Os métodos de diagnósticos convencionais e as opções de tratamento para o carcinoma urotelial do trato urinário superior (UTUC) são baseados nos critérios estabelecidos para o cancro da bexiga devido à falta de conhecimento acerca da gestão da doença. Os pacientes são frequentemente submetidos a procedimentos invasivos e desconfortáveis durante o período de monitorização da doença. Assim, alternativas não invasivas são uma necessidade urgente, mas ainda não atendida. Estudos genómicos e evidências moleculares mais robustas são necessários para identificar subgrupos moleculares com vias distintas de patogénese, que podem ter implicações prognósticas e terapêuticas no carcinoma urotelial do trato superior.

O objetivo principal deste estudo é caracterizar geneticamente uma série de UTUC e esclarecer o uso potencial de biomarcadores genéticos no tratamento e prognóstico da doença. Nesse sentido, procedemos ao estudo mutacional dos genes FGFR3, TERTp e RAS numa série selecionada de pacientes com UTUC e estabelecemos correlações entre as características clínico-patológicas e os dados moleculares. Além disso, planeámos avaliar a expressão de marcadores de imunohistoquímica (CK5/6 e CK20) para diferenciar subtipos moleculares clinicamente relevantes.

Um estudo coorte de pacientes com diagnóstico confirmado de UTUC foi selecionado para caracterização molecular. Blocos de tecido FFPE foram seccionados para análise da expressão genética e imunohistoquímica. O perfil mutacional do tumor foi avaliado para os genes FGFR3 e TERTp por qPCR, enquanto os genes RAS (HRAS, KRAS e NRAS) foram avaliados por PCR e sequenciação de Sanger. O painel de imunohistoquímica foi composto por marcadores basais (CK5/6) e luminais (CK20).

Análises univariada e multivariada foram realizadas para estimar correlações entre as características clínico-patológicas e moleculares de amostras de tecido tumoral, usando a versão mais recente do SPSS.

Em 141 amostras de UTUC, 106 (75,2%) apresentavam mutação em pelo menos um dos genes estudados. Nesta coorte, foram encontradas as seguintes frequências de mutação: 55,5% para *FGFR3*, 54,2% para *TERT*p, 6,4% para *KRAS*, 2,1% para *HRAS* e 0,7% para *NRAS*. No presente estudo, observámos que a invasão venosa foi o único fator preditivo de metástase à distância e que as mutações no *FGFR3* foram estatisticamente associadas à ausência de invasão linfática e venosa, denotando o seu efeito como marcador de bom prognóstico. Mutações no *NRAS* foram associadas a idades mais jovens, embora apenas uma mutação tenha sido identificada. Não foram encontradas associações entre os dados

clínico-patológicos e outras alterações *RAS* ou *TERT*p. Alterações concomitantes entre os genes FGFR3 e TERTp foram estatisticamente significativas, tal como esperado.

Na maioria dos tumores, observámos um padrão de expressão aberrante de CK5/6 e CK20, estendendo-se além das camadas basal/intermediária e luminal, respetivamente. Comparando os graus histológicos, observámos que todos os casos com expressão negativa (0) para CK5/6 e CK20 e todos os casos com mais alta expressão eram tumores de alto grau. Estes resultados são ainda preliminares e estudos complementares (por exemplo, expressão de GATA3) serão necessários para uma melhor caracterização de subtipos moleculares em UTUC e sua eventual correlação com os dados moleculares e prognósticos

Palavras-chave: Alterações moleculares | Carcinoma urotelial do trato urinário superior | Marcadores de imunohistoquímica | Perfil mutacional

Introduction

1. Upper urinary tract system: embryology, anatomy, and histology

The human urinary system represents a contiguous group of organs with distinct anatomical features and several critical and coordinated functions such as excretion of toxic substances and metabolic products, homeostasis (in coordination with other organ systems), regulation of arterial pressure, and collection, transportation and temporary urine storage (**Figure 1**) [1, 2].

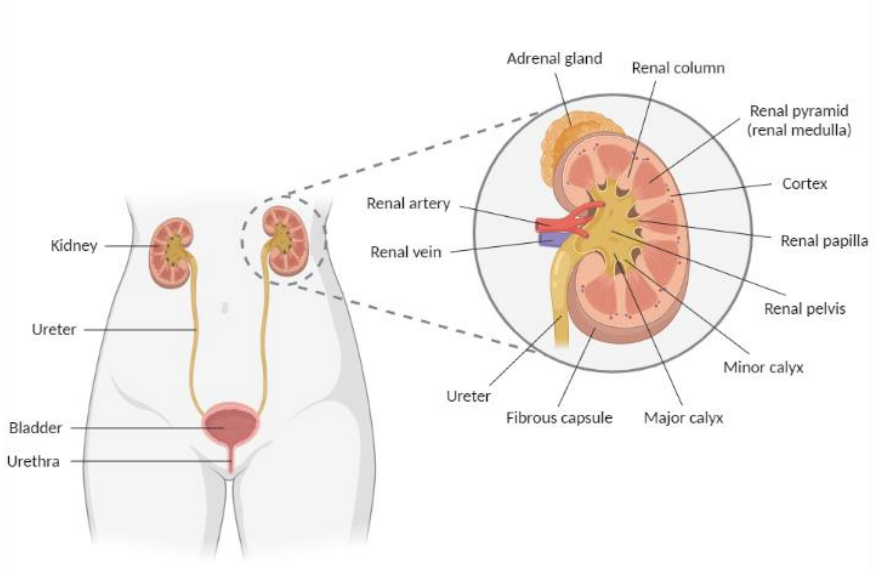

Figure 1. Urinary tract in the female abdomen with a labeled kidney cross-section. The kidneys and ureters are considered structures from the upper urinary tract whereas the bladder and urethra are both lower urinary tract structures [3]. Created with BioRender.com.

The mammalian upper urinary tract, which entails the pelvicalyceal system of the kidney and the ureter, begins its development at the 4th week of gestation and derives from a series of intermediate mesodermal structures (the pronephros, the mesonephros and the metanephros/definitive kidney), formed in temporal and spatial sequence that extend over the dorsal wall of the embryo [2-7]. In contrast, the lower urinary tract derives from embryonic endodermal structures [2, 7].

The kidneys are considered key regulators of tissue and body metabolism. They excrete unwanted substances from the blood (urea, metabolites, and other toxic products) to the urine, maintain homeostasis and regulate electrolyte composition of body fluids as well as arterial pressure [1, 6, 8, 9]. They are paired parenchymatous organs, situated on either side of the vertebral column and secured in the retroperitoneal space of the posterior abdominal wall by adipose (perirenal fat) and fibrous tissues [1, 10-12]. Each kidney is

supplied with blood by a renal artery, arising directly from the abdominal aorta, and drained by a renal vein, directly to the inferior vena cava [4, 12].

The kidneys constantly vary their weight and size depending on the volume of blood and urine they store. In normal conditions, each adult kidney measures around 11 cm in length, 6 cm in width and 3 cm in thickness. Male kidneys weigh around 150 g, while female kidneys weigh 10 to 15 g less [1, 6, 11-13].

The kidneys present three distinct regions: renal cortex, renal medulla, and renal pelvis. The cortex represents the outer layer of the kidney, while the medulla represents the inner layer. The latter contains renal pyramids, separated by renal columns, which drain to the renal papilla and form the minor calyces (**Figure 1**) [2, 12].

1.1. Renal Pelvis

In the human kidney, the compartment between the calyces and the ureter is called renal pelvis [5, 14, 15]. This cavity can greatly vary in size since it is responsible for collecting urine and can store it up to 10mL [1, 12].

More specifically, peristaltic contractions of the renal pelvic wall promote an active discharge of urine from the collecting ducts (at the renal papilla) into the minor calyces. These, in turn, expel urine into the major calyces to be collected by the renal pelvis and transported out of the kidney through the ureters [1, 2, 5, 14, 15].

1.2. Ureters

The ureters are contractile fibromuscular tubular structures that connect the renal pelvis to the urinary bladder, actively transporting urine produced by the kidneys. Peristaltic waves, spread to the renal pelvis, propel the final urine downward through the ureters and into the bladder for temporary storage [1, 2, 4, 5, 12]. After muscle relaxation, urine is released and expelled out of the human body through the urethra [1].

In the average adult, these bilateral structures are generally 25-30 cm in length, depending on the height of the individual, and course through the retroperitoneum. The ureter features three segments of similar length: an abdominal segment (also referred as proximal ureter) located on the posterior abdominal wall, a pelvic segment (also referred as middle ureter) located in the pelvic cavity and an intramural segment (also referred as distal ureter) where the ureter ends in the bladder. It also presents three clinically relevant areas, considered the most common locations for obstructions: an ureteropelvic junction (where the ureter joins with the renal pelvis), at the pelvic brim where the ureter crosses the iliac vessels, and an ureterovesical junction (where the ureter adjoins the bladder) [1, 2, 4, 5, 12, 13, 16].

Histologically, the pelvic and ureteric wall feature a transitional epithelium and an inner mucosal layer of connective tissue (lamina propria). Below the mucosa, the smooth muscle layer is responsible for the alternating peristaltic movements of the renal pelvis and the ureter, and externally the adventitial layer, which contains adipose and loose connective tissues, is responsible for supplying these structures with lymphatic and blood vessels and adhering them to the peritoneum (**Figure 2**) [1, 5, 7, 12, 17].

Typically, the renal pelvis and the proximal portion of the ureter contain only two thin muscular layers (inner longitudinal and outer circular), while the distal portion of the ureter as well as the urinary bladder comprised three muscular layers (inner longitudinal, middle circular and outer longitudinal) (**Figure 2**) [4, 18].

The superficial layer of the urothelium contains multinucleated and fully differentiated "umbrella" cells that contact with pyriform cells from the intermediate layer. The basal layer contains darkly stained and highly proliferative cells. These last two layers replace damaged umbrella cells, which continuously regenerate from urothelial stem cells supposedly residing in the basal layer.

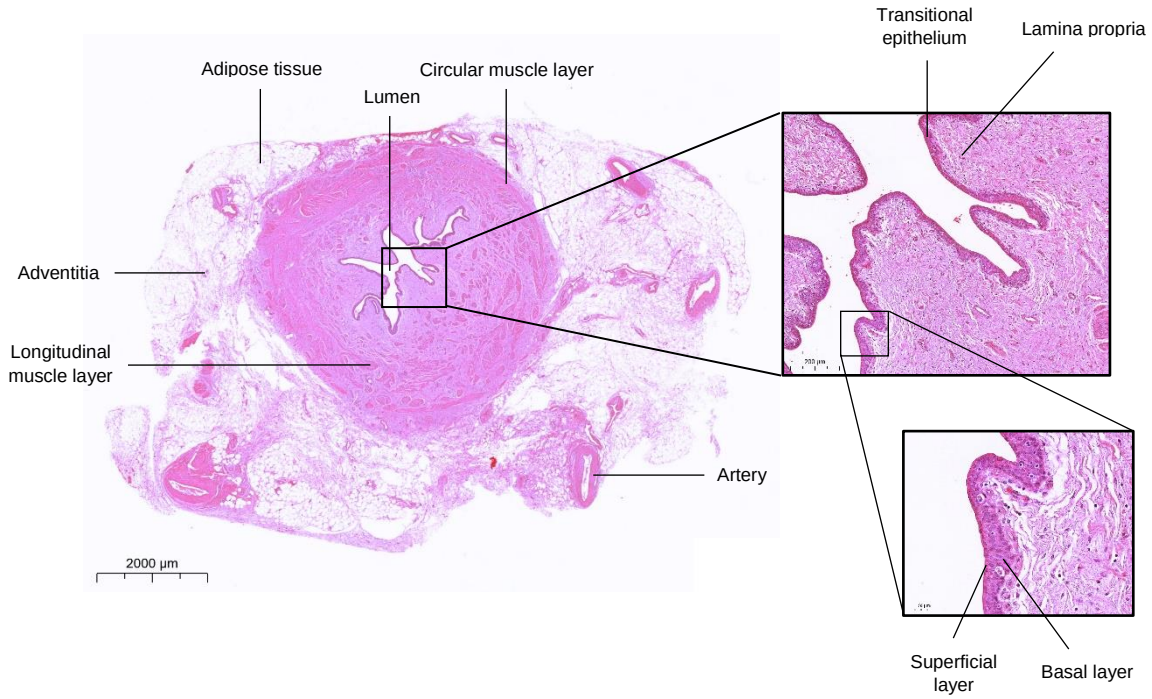

Figure 2. Transverse section of a ureter (Hematoxylin-eosin staining). Scale bar of 2000 µm, 200 µm and 50 µm.

2. Upper urinary tract urothelial carcinoma: epidemiology

Malignant epithelial tumors of the renal pelvis and ureter can be classified into adenocarcinoma (<1%), squamous cell carcinoma (~10%) and transitional cell carcinoma (urothelial carcinoma), which accounts for the majority of UTUCs (>90%) [4, 12, 19, 20].

Urothelial carcinoma (UC), from the upper and lower tract, represents the fourth most common form of cancer and the second most common genitourinary malignancy worldwide [21, 22].

Upper tract urothelial carcinoma (UTUC) arises in the urothelial cells lining the urinary tract from the calyceal system to the distal ureter [19, 23-25]. UTUC is a relatively rare urological malignancy, currently comprising 5-10% of urothelial tumors and less than 10% of renal tumors. At diagnosis, pelvicalyceal tumors are twice more common than ureteral tumors [19, 21, 22, 26-29].

This pathology predominantly affects Caucasian men, particularly between 70 to 90 years of age, with an incidence up to threefold higher than in women. In the past decades, the mean age of occurrence increased from 68 to 73 years [7, 21, 26, 30, 31].

Compared to urothelial cancer of the bladder (UCB), which accounts for most urothelial tumors (90-95%) [7, 32, 33], UTUC is biologically more aggressive and is associated with a worse prognosis. Overall, up to 60% of the patients with UTUC present muscle invasion (≥pT2) at diagnosis compared with 15-25% of patients with bladder cancer [21, 23, 34, 35]. Difficulties in early diagnosis, due to anatomical differences, such as thinner muscle layers and absence of serosa in upper tract structures, as well as genetic profile, could explain these differences [18, 19].

An accurate determination of UTUC incidence and etiopathogenesis is limited since they are often combined with other urinary pathologies such as kidney and bladder cancer [22, 23, 25, 33, 36]. Therefore, UTUC pathogenesis and clinical management are often extrapolated from well-established evidence observed in UCB [25, 32].

Using the National Cancer Institute's Surveillance, Epidemiology, and End Results (SEERS) database, Raman *et al.* demonstrated that the overall incidence of UTUC increased from 1.88 to 2.06 new cases per 100.000 inhabitants over the last decades [21, 26, 37]. This gradual increase was mostly due to a rise in the incidence of ureteral neoplasms (0.69 to 0.91 cases per 100.000 inhabitants) [7, 26, 35, 37]. However, advancements in imaging and endoscopic technologies and improvements in bladder cancer survival could also explain this observed increase [23, 37].

In Portugal, according to the most recent national data from *Registo Oncológico Nacional* (2010) [38], the incidence rate for renal pelvis malignancy was 0.6 per 100.000 inhabitants (0.3/100.000 in women and 0.9/100.000 in men) and for ureteral malignancy was 0.5/100.000 inhabitants (0.3/100.000 in women and 0.6/100.000 in men).

3. Upper urinary tract urothelial carcinoma: etiology

Besides from an increase in the incidence of ureteral tumors, several other factors have been postulated to explain the epidemiologic patterns observed in UTUC [23, 37].

3.1. Risk factors

In developed countries, cigarette smoking is the major and most significant risk factor for developing UTUC and is dependent on dose and duration of exposure [7, 19, 21, 32, 39, 40]. Another common risk factor includes occupational exposure to aromatic amines used in industrial chemicals (e.g., dye, textile, plastic and petroleum industries) [7, 19, 21, 32, 41].

Although the majority of UTUCs is sporadic, genetic conditions can also increase the risk to develop the disease. Patients with Hereditary Non-Polyposis Colorectal Carcinoma (HNPCC), due to germline mutations in DNA mismatch repair genes and microsatellite instability, account for 10-20% of all UTUCs and often present worse prognosis [7, 21, 31, 32, 42-44]. At presentation, these patients are diagnosed at a younger age with a higher female proportion [7, 32, 44].

Analgesic abuse and aristolochic acid ingestion (neurotoxin produced by the plants *Aristolochia fangchi* and *Aristolochia clematitis*), which can cause chronic kidney diseases such as Balkan Endemic Nephropathy (BEN) and Aristolochic Acid Nephtropathy (AAN), are risk factors specific to UTUC development [19, 21, 32].

About 80% of the patients with UTUC have a history of bladder cancer, which is also a relevant predisposing factor [19, 20, 24].

3.2. Symptoms

At diagnosis, most patients present macroscopic or microscopic hematuria (70-80%). Flank pain is also a common presenting symptom in this disorder (20-30%), usually caused by hydronephrosis which is the gradual obstruction of the kidney and/or ureters. Systemic symptoms (e.g., anorexia, weight loss, fatigue, bone pain, night sweats) are uncommon but often associated with worse prognosis and metastatic disease [4, 19, 21, 23, 32, 45].

4. Upper urinary tract urothelial carcinoma: clinical management

Urothelial cancer is considered one of the costliest cancers worldwide and a burden for the health care system, mostly due to lifetime surveillance and constant clinical examinations.

Despite its lower incidence, UTUC still remains an heterogenous and aggressive disease, often requiring invasive therapeutic procedures with high morbidity rates. The presentation of symptoms, such as hematuria, is the most common indicator of an upper

tract tumor and requires a full workup (detailed clinical history, physical examination, urinalysis, urine cytology, and imagining/endoscopic techniques) to establish a correct diagnosis [23, 25, 31, 37]. A cystoscopic evaluation is also relevant to visualize the lower urinary tract and exclude the possibility of synchronous bladder tumors [4, 19, 21, 46].

Computed tomography urography (CTU) remains the gold-standard imaging technique for the diagnosis of UTUC due to its high diagnostic accuracy and availability, replacing the previous method - intravenous pyelography [4, 19, 21, 25, 31, 34, 46, 47]. If radiation or iodinated contrast are contraindicated, magnetic resonance (MR) urography is the best alternative for the patients [19, 21, 23, 31, 34, 46, 47]. Flexible ureteroscopy allows the examination of the entire upper urinary tract and the immediate biopsy of suspected lesions, guiding risk stratification and treatment procedures [19, 21, 23, 31, 34, 37, 46, 48].

After establishing a correct diagnosis, clinical management and therapeutic strategies are established by risk stratification and survival outcomes [21, 31, 49]. Non-muscle invasive disease presents a 5-year cancer specific survival of 90%; however, for muscle-invasive disease, these rates decrease to less than 50% for pT2/pT3 stages and less than 10% for pT4 stage [7, 21, 26, 37, 45].

Radical nephroureterectomy (RNU) with excision of the bladder-cuff is the gold-standard treatment for high-risk non-metastatic UTUC [4, 19, 21, 25, 34, 50]. In contrast, low-risk patients are submitted to a more conservative approach, such as kidney sparing surgery, typically performed through an endoscopic procedure (i.e. ureteroscopy) [4, 19, 21, 25, 31, 34, 45, 50, 51].

Regarding metastatic disease, cisplatin-based chemotherapy seems to be effective as a first-line treatment. Additionally, immunotherapy with checkpoint inhibitors is a novel therapy regarded as a possible alternative for cisplatin-ineligible patients. Five agents (nivolumab, pembrolizumab, atezolizumab, avelumab and durvalumab) were approved by FDA, all directed to programmed cell death protein-1 (PD-1) and programmed cell death ligand-1 (PDL-1) [21, 49, 52].

However, even after surgery, UTUC presents high recurrence and progression rates, particularly in patients with low-grade disease submitted to conservative procedures. Therefore, they require frequent and intense lifetime surveillance to detect concomitant tumors, intravesical recurrences or distant metastases [21, 25, 31, 34, 45, 51].

The European Association of Urology Guidelines recommend cystoscopy and urine cytology (with an indication of CTU) with close vigilance for the first two years and then annually for at least five years. Patients that underwent a conservative procedure require a stricter protocol [21, 25, 34, 53].

The lack of non-invasive methods to diagnose and follow urothelial cancer is an ongoing problem. It's imperative to advance the current imaging techniques and acquire novel diagnostic procedures to detect tumors in earlier stage/grade and improve prognosis [21, 49]. Additionally, understanding of the genomic profile of UTUC has the potential to develop individualized therapies, targeted to specific alterations present in each tumor but also the potential to improve the detection of recurrent tumors.

5. Upper urinary tract urothelial carcinoma: prognostic factors

Similar to bladder cancer, several prognostic factors can impact UTUC prognosis and outcome. As discussed below, some are related to patient and tumor features, while others are related to clinical management and surgical options.

5.1. Clinical factors

Smoking status is widely accepted as the main risk factor. It also increases the risk of recurrence and mortality in urothelial cancer. Compared to non-smokers, lifetime smokers (more than 20 cigarettes per day with more than 20 years of exposure) present an increased risk of cancer-specific mortality and intravesical recurrence [19, 21, 45, 54, 55]. It has been demonstrated that smoking cessation could decrease the risk of UTUC development and improve its outcome [19, 21, 40, 54].

As previously mentioned, UTUC incidence is predominantly observed in elderly patients. Advanced age has been associated as a predictor of aggressive disease, decreased cancer-specific survival and intravesical or loco-regional recurrence [21, 45].

Some epidemiologic studies demonstrated worse prognostic features and lower survival rates in female and nonwhite individuals, specifically black non-Hispanic patients [7, 23, 37, 45, 55]. However, unlike bladder cancer, both gender and ethnical background remain controversial topics in the literature, not yet established as independent predictors of survival in UTUC patients [7, 19, 21, 23, 26, 30, 51, 55].

Several other clinical factors, such as the presence of hydronephrosis, obesity (defined as body mass index ≥ 30 kg/m^2), systemic symptoms and previous/ synchronous bladder cancer are established predictors of advanced disease and worse outcomes in UTUC patients. They often present more biologically aggressive features [19, 21, 26, 45, 55-57].

The impact of the location of the primary tumor in prognosis is an ongoing debate [19, 26, 29, 45, 55, 58]. Compared to renal pelvis tumors, some authors have reported more aggressive phenotypes and worse prognoses in ureteral tumors, while others found no significant differences regarding survival and disease recurrence [19, 21, 26, 28, 55, 58-61].

The molecular profile of UTUC patients is also still an ongoing work. Although recent authors described various associations between prognostics factors and genetic/epigenetic alterations, more validation studies are required for their use in clinical practice (see below) [7].

5.2. Pathological factors

Pathological stage is the best-established predictor of survival in UTUC patients, expected to present worse prognosis with increasing tumor stage [21, 35, 45]. Histological grade and tumor size have also shown correlation with stage and cancer-related outcomes [21, 35, 45].

Multifocal tumors are defined as the presence of two or more distinct locations within the urothelium. If renal pelvis and ureter are both affected, a poorer prognosis is expected with higher disease recurrence and cancer specific-mortality [19, 21, 45, 61].

Tumor architecture (sessile lesions are associated with loco-regional recurrence and lower cancer-specific survival), extensive necrosis and lymphovascular invasion (present in approximately 20% of UTUCs) are valuable and reliable tumor related factors, which have been established as adverse predictors of UTUC prognosis and should aid clinical management [19, 21, 35, 45, 55, 62, 63].

5.3. Surgical factors

Surgical delay for tumor removal, specifically RNU, was associated with aggressive biological features and increased risk of disease progression [19, 21, 45]. Also, surgical approach (laparoscopic RNU versus open RNU) can have an impact on recurrence and disease progression; in this case, LRNU is a less invasive alternative and seems to deliver more effective results [19, 45, 55].

Although lymph node dissection (LND) is still controversial and not standardized treatment, high-risk patients appear to benefit with this surgical approach [19, 21, 45, 64].

6. Upper urinary tract urothelial carcinoma: staging, pathology and morphology

Upper tract cancer is a highly heterogenous disease with distinct pathways of pathogenesis between papillary and non-papillary tumors. UTUC and UCB share similar morphological features and classification systems, further discussed in the following sections [19, 21].

6.1. Tumor, node, metastasis staging

Regarding primary tumors (T), the tumor, node, metastasis (TNM) staging system defines non-invasive lesions (invasion within the lamina propria) as flat non-invasive

carcinoma *in situ* (CIS/Tis) and non-invasive papillary carcinoma (pTa). Invasive lesions are subdivided into the following categories: pT1 - tumors that invade the subepithelial connective tissue; pT2 - tumors that invade the muscularis; pT3 (renal pelvis) - tumors that invade into peripelvic fat or renal parenchyma; pT3 (ureter) - tumors that invade into periureteric fat; and pT4 - tumors that invade into adjacent organs or through the kidney into perinephric fat [19, 21, 49, 65, 66].

Additionally, regional lymph nodes (N) can be classified into NX (regional lymph nodes unable to be assessed), N0 (no regional lymph node metastasis identified), N1 (metastasis in a single lymph node, ≤2 cm in greatest dimension), N2 (metastasis in a single lymph node, 2-5 cm in greatest dimension; or in multiple lymph nodes, <5 cm in greatest dimension) and N3 (metastasis in a single lymph node, >5 cm in greatest dimension). Distant metastasis (M) is described as either M0 (no distant metastasis) or M1 (presence of distant metastasis) [21, 66].

6.2. Histopathological grading

The 2016 WHO/ISUP classification distinguishes papillary urothelial neoplasia into four major categories, according to the tumor's architectural and cytological features. Urothelial papilloma (a precursor of papillary tumor) is considered a benign lesion, while papillary urothelial neoplasm of low malignant potential (PUNLMP), low-grade (LG) papillary urothelial carcinoma, and high-grade (HG) papillary urothelial carcinoma are considered lesions with malignant potential [19, 21, 67, 68].

PUNLMP presents a thickened urothelium with abnormal cellular proliferation and minimal architectural and cytological changes. Compared to low and high-grade tumors, this is an extremely rare tumor with low recurrence rates and very low propensity to progress in stage and grade; therefore, with a particularly good prognosis [19, 67, 69, 70].

Low-grade carcinomas are characterized by distinct cytological abnormalities with some architectural disorder [19, 66, 67]. These tumours account for 20-30% of all UTUCs and rarely invade; however, follow-up procedures are frequently required due to their high recurrence rates [68, 69]. Only 10-15% of low-grade tumors eventually progress to high grade invasive carcinoma, mostly due to the acquisition of *TP53* mutations [20, 68, 71].

In contrast, high-grade carcinomas represent the most common tumors in upper tract (70%) and are characterized by complex architectural and cytological abnormalities with an atypical epithelium and loss of polarity [19, 66, 67]. They present high recurrence rates but, unlike low-grade tumors, they rapidly progress to invasive stages [66, 68, 69]. This often reflects a poor clinical prognosis and resistance to therapy.

6.3. Molecular subtypes

6.3.1. Classification based on depth of invasion

Non-muscle invasive carcinoma (NMIC) most often presents itself as a papillary tumor, presenting a relatively low risk of progression to invasive disease and low cancer-specific mortality. However, since they tend to recur quite frequently, lifetime surveillance is mandatory for these patients [52, 72, 73]. Almost all non-muscle invasive carcinomas are classified as low-grade tumors and frequently acquire FGFR3 activating mutations, which confer a favorable prognosis but higher risk of recurrence [49, 72]. Together with RAS mutations, these are early events in carcinogenesis and often mutually exclusive [49, 74-76].

Muscle-invasive carcinoma (MIC) is a clinically aggressive non-papillary tumor that arises from flat dysplasia or carcinoma *in situ* but rarely arises from papillary tumors. As a high-grade tumor, it rapidly progresses and often develops metastatic disease, predicting an adverse outcome in these patients [49, 52, 72, 73]. Prognosis and clinical management will differ according to the depth of invasion that characterizes each tumor. This lethal phenotype can present alterations in FGFR3 but in a much lower frequency than NMIC. Instead, genomic instability and inactivating mutations in tumor suppressor genes such as TP53 and retinoblastoma (RB1) are the major alterations observed in this subtype which are associated with worse prognosis [19, 49, 66, 72].

NMIC corresponds to the initial stages of pathogenesis (Tis, Ta and T1), while stages that invade beyond the muscle layer (T2, T3 and T4) belong to MIC [21, 49]. Interestingly, carcinoma *in situ* is considered a high-grade tumor mostly due to its poorly differentiated nature and the early presence of TP53 mutations, presenting a higher propensity to progress to invasive stages [49, 65].

6.3.2. Classification based on molecular markers

Recently, other definitions were postulated for bladder cancer, according to the molecular characterization of each tumor.

As previously mentioned, the normal urothelium presents three distinct layers of cell differentiation. The heterogeneity of bladder tumors helped identify certain markers with expression patterns specific to each cell layer [71, 72]. Several studies established hierarchical clusters, using gene expression and mutational profiles, that could stratify bladder cancer into at least two major subtypes (basal and luminal), in analogy to what was originally identified in human breast cancer [52, 71-73, 77-79].

These intrinsic subtypes showed distinct clinical behaviors and responses to therapy while also predicting clinical outcome and cancer progression [52, 71, 73, 77]. Due to its

clinical relevance, basal squamous and luminal papillary subtypes were also mentioned for upper tract cancer. However, more validation reports are required to make an accurate assumption on UTUC prognosis.

In 2017, The Cancer Genome Atlas (TCGA) reported 5 molecular subtypes for muscle-invasive bladder cancer: luminal papillary (35%), luminal infiltrated (19%), luminal (6%), basal squamous (35%), and neuronal (5%). Additional subtypes have been recognized by other cohorts; for example, “double negative” (lack of expression of luminal and basal biomarkers) and “p53-like” (upregulated expression of p53 target genes) tumors [52, 71-73, 77-79].

Although luminal papillary tumors respond poorly to chemotherapy, they retain the best survival outcomes [52, 72]. Therapy with FGFR inhibitors is an alternative clinical approach due to the high frequency of FGFR3 alterations in these tumors [49, 52, 72, 79]. They also display an “immune desert” phenotype, deriving the least benefit from immunotherapy. However, that doesn’t occur with other luminal tumors, referred as “luminal-infiltrated”, which are also chemoresistant but seem to respond to immune checkpoint inhibitors [72, 73, 77-79]. Additionally, it has been demonstrated that UTUCs have a predominant luminal-papillary phenotype [80].

Basal squamous tumors appear to be intrinsically more aggressive with higher propensity to invade and metastasize than luminal tumors. However, prognosis can be improved if patients are submitted to aggressive clinical management [71-73, 77-79]. They are thought to develop from a non-papillary pathway and appear to be enriched with squamous differentiation features and immune checkpoint markers (PD-L1 and CTLA-4); therefore, they are likely to respond to immunotherapy [71, 73, 77-79].

Although disparities in terminology have been present over the years, the set of immunohistochemical markers for the two main molecular subtypes is similar among different studies [52, 71, 73, 77-79]. The basal cluster is characterized by a strong expression of stem cell markers such as CD44 and high molecular weight keratins (KRT5, KRT6A and KRT14), while the luminal cluster expresses high levels of urothelial differentiation markers such GATA3, FOXA1, KRT20 and uroplakins [52, 71, 73, 78, 79].

7. Upper urinary tract urothelial carcinoma: molecular markers

In the past decades, knowledge on the molecular mechanisms of UTUC was severely lacking due to the rarity of this disease [81]; however, recent studies have focused on molecular markers for their potential to guide patient risk stratification, clinical management and, ultimately, contribute to a more comprehensive understanding of UTUC. Additionally,

these biomarkers could promote more personalized and selective diagnosis/prognosis strategies, avoiding unnecessary invasive procedures and improving disease surveillance, prognosis and morbidity. They could also constitute novel target-based therapies [52, 65, 73, 82]. Due to its importance in a preclinical setting, the genomic profiling of primary and metastatic UTUC should be considered for implementation in the clinical practice.

As previously mentioned, urothelial carcinoma is a highly heterogenous disease, developing and progressing through the accumulation of epigenetic and genetic alterations [52, 65, 73]. Currently, UTUC and UCB are considered distinct entities with several clinical and biological differences. They share similar molecular alterations, but critical differences are observed regarding their prevalence [81]. The most common pathogenic alterations will be discussed in detail in the following sections.

7.1. Mitogen-activated protein kinase (MAPK) signaling pathway

The mitogen-activated protein kinase (MAPK) signaling pathway, specifically involving the extracellular signal-regulated kinases (ERK), is the most frequent altered pathway in urothelial carcinoma [65, 83]. It plays a significant role on the regulation of diverse cellular responses such as proliferation, differentiation, migration, survival and apoptosis [82-86].

An external factor (hormones, chemokines or growth factors) promotes the initiation of this pathway through stimulation of the tyrosine kinase receptors (TKRs), present on the cell membrane. Ligand binding promotes a receptor conformational change that results in the activation of RAS which in turn activates a cascade of interconnected protein kinases (RAF1/MEK/ERK). These serine-threonine kinases phosphorylate and activate each other sequentially and function as signal transducers between the extracellular and intracellular environment [82-85, 87, 88]. Inside the nucleus, they transactivate transcription factors and regulate gene expression (**Figure 3**) [82, 85, 87-89].

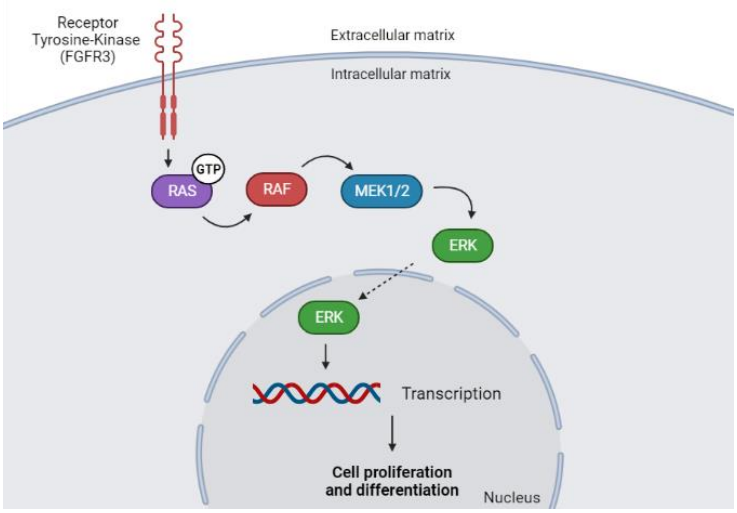

Figure 3. The ERK MAPK signaling pathway. The MAPK signaling pathway is initiated when an external factor/ligand binds to the tyrosine-kinase receptor and promotes receptor dimerization and activation of a RAS G-protein. The "on" state of RAS leads to the activation of RAF proteins which begins a downstream cascade of kinases. After interaction with MEK, activated ERK enters the cell nucleus and regulates gene expression and protein synthesis. Created with BioRender.com.

Dysregulation and downstream activation of the MAPK pathway through molecular alterations in members of this signaling cascade, i.e. amplification and activating mutations in cell surface receptors or in intracellular signal transducers, occurs in approximately 30% of human cancers [65, 82, 84, 86, 89, 90]. *RAS* and *FGFR3* mutations, usually mutually exclusive events in cancer, are known to be pathogenic and occur in 85% of low-grade urothelial carcinomas [74, 75, 91]. Therefore, several studies have focused on understanding the impact of this pathway on UTUC tumorigenesis and, subsequently, as a potential therapeutic target to improve patient survival and prognosis.

7.1.1. *FGFR3* mutations

The fibroblast growth factor receptors (FGFR) are a highly conserved family of TKRs, responsible for interacting with growth factors and upregulating the MAPK signaling pathway [52, 74, 92, 93]. These cell membrane receptors are glycoproteins composed of a hydrophobic transmembrane domain, which separates the intracellular tyrosine kinase domain from the extracellular ligand-binding domain (**Figure 4**) [74, 91, 93]. After fibroblast growth factors (FGFs) bind to their receptor through the extracellular domain, receptor dimerization and transphosphorylation of the tyrosine kinase domain trigger downstream activation of the MAPK signaling pathway [74, 92, 93].

Four distinct genes have been described (FGFR1-4), of which *FGFR3* is located at the human chromosomal locus 4p16.3. FGFR3 signaling has a preponderant role in physiological processes such as embryogenesis and skeletal development, proliferation, angiogenesis, and survival [74, 92, 93]. This proto-oncogene is frequently overexpressed in malignant neoplasms through point mutations, gene amplification or chromosomal translocations. The most common missense mutations affect the extracellular domain of the FGFR3 protein (exon 7) at codons 248 and 249 (p.R248C and p.S249C, respectively), the latter being considered the most prevalent hotspot mutation (**Figure 4**) [74, 76, 93]. These gain-of-function alterations result in novel cysteine residues which lead to ligand-independent receptor dimerization and constitutive activation of FGFR3 signaling [74, 92]. During carcinogenesis, this translates into loss of control over cell growth and differentiation.

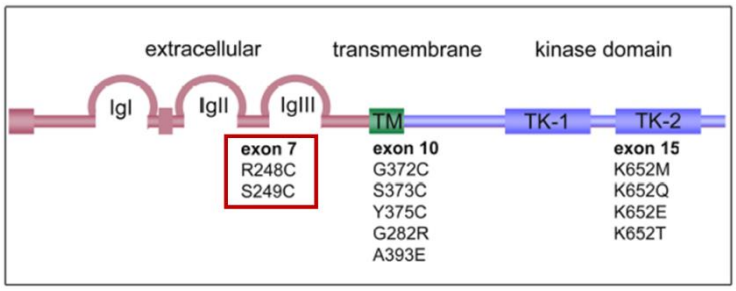

Figure 4. FGFR3 mutations lead to FGFR3 constitutive activation. FGFR3 is one of the tyrosine-kinase receptors of the MAPK signaling pathway and is activated by the binding of a growth factor, hormone or chemokine. Abnormal expression of FGFR3 occurs due to mutations on exon 7 of the extracellular domain, of which R248C and S249C are the most common (red box). Adapted from Knowles, M. A., World J Urol. (2007) [91], after permission request.

Somatic mutations in *FGFR3* are common events in urothelial cancer, reported in 60-80% of non-muscle invasive bladder carcinomas and up to 20% of muscle invasive disease [52, 65, 74, 76, 93, 94]. Due to its low frequency in invasive disease, studies have proposed a protective role of FGFR3 mutations on tumor progression (REFS). Moss et al. reported a mutation rate of 92% in low-grade and low-stage tumors of the upper urinary tract. Although not as high, a significant proportion of high-grade UTUCs was also found mutated for *FGFR3* (60%) [74, 81]. Alternatively, these alterations could represent early genetic event during carcinogenesis since it was reported *FGFR3* mutations in urothelial papilloma [74, 91].

As previously mentioned in section **6.3.**, FGFR3 alterations were associated with less aggressive disease and better survival in invasive urothelial carcinoma; however, a higher disease recurrence is observed in these patients [65, 74, 92, 94, 95].

7.1.2. *RAS* mutations

Rat sarcoma viral oncogene homolog (RAS) is a family of small G-proteins that function as GTPases at the inner surface of the cell membrane [82, 86, 88]. While guanine nucleotide exchange factors (GEFs) promote an active state of RAS by catalyzing guanosine diphosphate (GDP) dissociation and rebinding guanosine triphosphate (GTP) to TKRs, GTPase-activating proteins (GAPs) are responsible for an “off” state by stimulating the hydrolysis of GTP to GDP; therefore, deactivating the kinase activity of the MAPK and PI3K-AKT signaling pathways [82, 83, 85, 88, 96].

RAS isoforms are highly homologous proteins of 21kDa, encoded by three ubiquitously expressed genes: KRAS, HRAS and NRAS [82, 83, 86, 88, 96]. *KRAS* is located at 12p12.1, *HRAS* is located at 11p15.5 and *NRAS* is located at 1p13.2 genomic regions [88, 90].

Point mutations in RAS isoforms are described as common oncogenic events in several types of cancer and mainly occur in codons 12/13 (exon 1) and 61 (exon 2) [76, 82, 84, 86, 90, 96]. Distinct mutational signatures have been reported according to each RAS isoform and type of cancer: KRAS mutations mainly affect codon 12 and are highly prevalent in pancreatic, colorectal and non-small cell lung carcinomas, while NRAS mutations are more commonly found in codon 61 and are frequent in hematologic malignancies, thyroid carcinomas and melanoma. HRAS seems to show a similar mutational pattern in codons 12 and 61 and frequently occur in bladder and kidney carcinomas [82, 90, 96]. These somatic alterations either decrease intrinsic GTPase activity of RAS proteins (codon 61 alterations) or increase their affinity to GTP-bound conformation (codons 12/13 alterations), yet both disrupt normal RAS inactivation. RAS over activation leads to aberrant cell signaling, even in the absence of external stimuli, and eventually to cell malignant transformation and tumor growth [82, 86, 90, 96].

All isoforms have been found mutated in urothelial cancer, although *NRAS* is the least detected proto-oncogene [76, 90]. In a recent study by Audenet et al [97], they reported HRAS mutations in 12% and 4% of UTUC and UCB cases, respectively. HRAS seems to be the most common mutated RAS gene in UTUC while KRAS and NRAS present similar mutational frequencies in both neoplasms [98]. Several studies have related mutant HRAS with a favorable prognosis, while KRAS genes were associated with a more aggressive clinical outcome; thus, also proposed as prognostic factors in urothelial carcinoma [86, 90].

7.2. h*TERT* mutations

Telomeres are nucleoproteins composed by non-coding 5´-TTAGGG-3´ hexanucleotide tandem repeats at the end of eukaryotic chromosomes, essential to preserve chromosomal stability and integrity [94, 99-102]. Telomerase is a ribonucleoprotein complex responsible for maintaining telomere homeostasis by adding telomeric tandem repeats to chromosomes and preventing the induction of apoptosis or cellular senescence [99-102].

The regulation of telomerase activity is essentially carried out by two subunits: the telomerase RNA component (TERC) and the human telomerase reverse transcriptase (hTERT), which is the catalytic protein subunit of telomerase [99, 101-103]. This enzyme is responsible for the extension of telomeric DNA and is encoded by the gene h*TERT* located on chromosome 5p15.33. Although TERC is expressed in most cell types, h*TERT* is constitutively expressed in germline and stem cells but transcriptionally repressed during the differentiation of most normal somatic cells. When telomerase is silenced, progressive shortening of telomeric DNA occurs after each cell division, until it leads to critical loss of genetic information and, ultimately, replicative senescence [94, 99-104].

Replicative immortality, through telomerase reactivation, is one of several well-established hallmarks of cancer and occurs in approximately 80-90% of malignant tumors [99, 103, 105]. Several mechanisms were proposed for telomerase activation including h*TERT* promoter mutations (either at the germline or at the somatic level), epigenetic alterations, h*TERT* amplification and alternative splicing [99, 101, 104, 106]. Telomerase activity occurs in normal proliferative cells of self-renewing tissues and it seems that aberrant hTERT expression is required in tumors from tissues with low capability of proliferation and regeneration [94, 100, 101, 106].

Mutations in the promoter region of hTERT have been identified in numerous cancer types, mainly in sporadic and adult tumors (central nervous system (43%), skin melanoma (29%) and thyroid cancer (10%)) [99, 101, 103, 104, 106, 107]. Particularly, they are well established events in urothelial cancer, reported up to 80% of UCB, independently of stage and grade [94, 99, 101, 104, 107]. Although not as frequently mutated in UTUC (approximately 50%) [99, 100], *TERT* has gained recent interest due to its potential as a molecular biomarker in early detection and follow-up of urothelial cancer [49, 99, 100, 107].

Two hotspot mutations are predominantly affected in the promoter of *TERT* (on chromosome 5), located at positions -124 base pairs (bp) (g.1295228 C>T) and -146 bp (g.1295250 C>T) upstream of the transcription ATG start site. Hereafter referred to as -124 C>T and -146 C>T, respectively [94, 99, 101, 103, 104, 106, 107]. These cytidine to thymidine (C>T) transitions are generally mutually exclusive events (with the exception of

skin cancers) and several studies have reported -124 C>T as the most prevalent hotspot mutation [94, 101, 103, 106]. They have been proposed as early genetic events on oncogenesis and they tend to co-occur with *FGFR3* alterations (**Figure 5**) [94, 101, 106, 107].

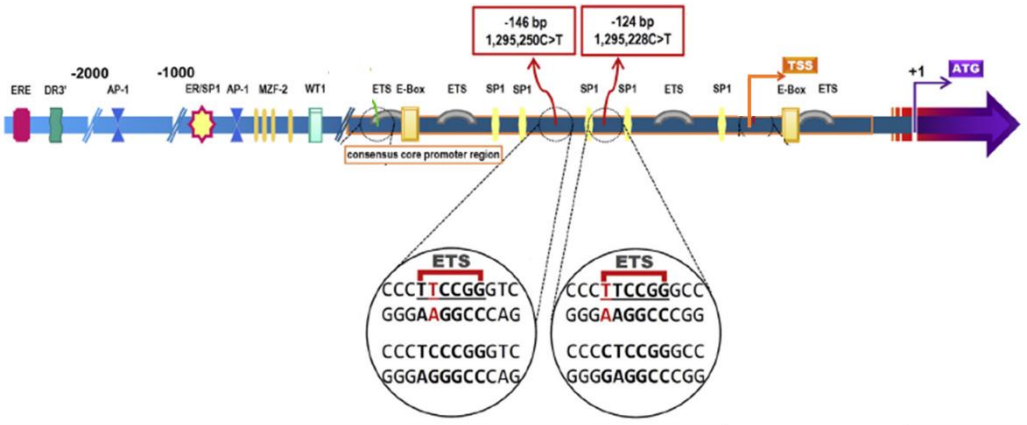

Figure 5. Mutations in the promotor of TERT lead to re-expression of telomerase in somatic cells. TERT promoter mutations, specifically at positions -124 bp and -146 bp upstream of the ATG start codon, generate a ligand binding site for ETS transcription factors which promote constitutive transcription of TERT and re-expression in somatic cells. They acquire the ability to continuously replicate and avoid cellular senescence. Adapted from Heidenreich B., Mutat Res/Rev Mutat Res (2017) [108], after permission request.

TERTp mutations are responsible for creating a consensus binding site (5'-GGAA-3') for E-Twenty-Six (ETS) transcription factors such as GABPA, which promotes *TERT* transcription and re-expression in somatic cells [94, 99, 101, 103, 104, 106, 107]. In this way, the telomerase complex is reactivated and previously normal somatic cells can now avoid cellular senescence and achieve replicative immortality by preserving telomere length and structure [99, 101, 107].

Associations between hTERT promotor mutations and aggressive clinical behavior have been proposed in various types of cancer. These include older age, higher risk of progression to invasive disease, worse response to therapy, distant metastasis, poor prognosis and higher risk of cancer-specific mortality [99, 101, 104]. However, some of these associations are still in debate for urothelial cancer; thus, it remains critical to understand the impact of these mutations on urothelial carcinogenesis, specifically for the improvement of individualized treatments and disease management as well as in a prognostic setting and patient risk stratification.

7.3. Immunohistochemical markers

Cytokeratins (CKs) belong to a family of intermediate filament proteins, expressed by epithelial and mesothelial cells and responsible for preserving both tissue and cell integrity and mechanical stability [109-113]. They are regarded as epithelial differentiation and maturation markers and present differences in terms of distribution and expression patterns [110, 112]. Several types of cancer acquire abnormalities in CK patterns; therefore, these cytoskeletal proteins have been proposed as diagnostic and predictive markers in carcinogenesis [109, 112, 114]. They appear to be effective surrogate biomarkers to predict and distinguish luminal from basal-like subtypes in urothelial cancer.

As previously mentioned in topic **6.3.2.**, studies have demonstrated that abnormal CK5/6 and CK20 expression were key features of the intrinsically aggressive basal subtype and chemoresistant luminal subtype of muscle invasive disease, respectively [78, 79, 110, 114]. Additionally, both cytokeratins were described as predictors of patient survival in non-muscle-invasive papillary high-grade UTUC since CK5/6-low/CK20-high was associated with a poor prognosis [113-115].

Cytokeratin 5 and 6 are type II cytokeratins, encoded by KRT5 and KRT6 (located on chromosome 12q13.13), respectively [113]. Normal expression of CK5/6 is restricted to the cytoplasm of basal and undifferentiated cells of the breast, prostate, urothelium and salivary glands [110, 111, 113, 114].

Cytokeratin 20 is a type I low-molecular weight cytokeratin, encoded by KRT20 (located on chromosome 17q21.2) [109, 113]. Normal expression of CK20 expression is observed in terminally differentiated urothelium, specifically in “umbrella” cells of the superficial layer. Less frequently, it can be found expressed in intermediate cells [109-114, 116].

Altered subcellular localization of CK20 such as staining in deeper or in all cell layers of the urothelium is hypothesized to correlate with altered urothelial differentiation during carcinogenesis [111, 113, 116]. Dysregulation of CK20 was proposed as an early event in the development of urothelial cancer due to its presence in non-invasive tumors [109, 111, 113, 114, 117]. It has also been proposed that loss of CK5/6 expression could represent a marker of poor prognosis in high-grade urothelial carcinomas [113].

Additionally, Harnden et al. suggested that tumors with normal CK20 staining were less likely to develop recurrences, which demonstrates its potential as a predictor of recurrence and behavior in urothelial tumors [116, 117].

Aims

The main aim of this project is to characterize the genetics of upper tract urothelial carcinoma (UTUC) and enlighten the potential use of genetic biomarkers in disease management and prognosis. In that regard, we will perform the molecular characterization of a series of upper urinary tract urothelial tumors through standard PCR, qPCR and immunohistochemistry, and correlate these findings with the clinicopathological features of the tumors.

Specifically, we aim:

(1) To characterize UTUC samples through the analysis of genetic biomarkers (TERTp, FGFR3, HRAS, NRAS and KRAS);

(2) To evaluate the expression of immunohistochemical markers (CK5/6 and CK20) to differentiate the background of clinically relevant UTUC molecular subtypes;

(3) To establish associations between clinicopathological variables and molecular data to improve prediction of prognosis.

Material and Methods

The following procedures were performed with the approval of the ethic committee, granted on February 3rd of 2020 (*Referência 425/19, Comissão de Ética para a Saúde do Centro Hospitalar Universitário de São João/Faculdade de Medicina da Universidade do Porto*).

1. Biological samples

The samples analyzed in this study were retrieved from a sequential series of patients with a confirmed diagnosis of upper urinary tract urothelial carcinoma (UTUC) and submitted to a surgical procedure in *Centro Hospitalar Universitário de São João* (CHUSJ), between the years 2009 and 2019, inclusive. One hundred and forty-one UTUC samples, corresponding to one hundred and fourteen patients, were reviewed by the same pathologist from CHUSJ and representative blocks were selected for molecular characterization. Those FFPE tissue samples corresponded to one hundred and twenty-five tumors, eight samples of associated epithelial lesions (CIS) and eight samples of lymph node (LN) metastasis. Relevant clinical and pathological characteristics are summarized in **Table 6** and **Table 7** of the Results section.

The inclusion criteria were adult patients ≥ 18 years-old; histologically confirmed diagnosis of UTUC and signed informed consent for patient participation in the study. Minor components (less than 50 percent) of variant histology such as glandular, squamous differentiation, sarcomatoid or micropapillary change were allowed as well as previous uro-oncologic history (previous or concomitant non-invasive, muscle-invasive carcinoma or carcinoma in situ of the bladder; previous intravesical chemotherapy or immunotherapy; and neoadjuvant or adjuvant chemotherapy for bladder cancer). Patients were excluded from the study if the following was observed: a predominant pure squamous or sarcomatoid variant histology in reviewed specimen; pathological finding consistent with small cell or neuroendocrine UTUC; inadequate clinical data from participants and lack of representative tumor sample.

2. Tissue Sections

FFPE tissues were sectioned using a paraffin microtome (Microm HM335E). Seven slides were obtained per case: one for hematoxylin-eosin staining (3-µm thick segments), three for immunohistochemistry (3-µm thick segments) and two for DNA extraction (10-µm thick segments).

3. Hematoxylin-eosin staining

Deparaffinization of the slides was accomplished with two consecutive incubations in xylol (Enzymatic, Santo Antão do Tojal, Portugal) for 10 minutes each, followed by hydration with decreasing concentrations of ethanol (Enzymatic, Santo Antão do Tojal, Portugal) for 5 minutes each: two consecutive incubations in 100% ethanol, one incubation in 96% ethanol, and one incubation in 70% ethanol. The slides were washed in running water for 5 minutes and stained with hematoxylin (DIAPATH, Martinengo, Italy) for 4:30 minutes. After rinsing in running water for 5 minutes to remove the excess of stain, the slides were re-immersed in ethanol 70% for another 5 minutes and stained with eosin-Y alcoholic (Richard Allan Scientific, ThermoScientific, Waltham, MA, USA) for 3 minutes. Tissue dehydration was accomplished using increasing concentrations of ethanol (Enzymatic, Santo Antão do Tojal, Portugal) for 5 minutes each: one incubation in 96% ethanol, and two incubations in 100% ethanol. Finally, two consecutive incubations in xylol for 10 minutes each were performed, and all slides were assembled with mounting medium (Richard Allan Scientific, ThermoScientific, Waltham, MA, USA).

4. DNA extraction, quantification, and quality assessment

The tumor area for manual microdissection was selected by the same pathologist at the Anatomical Pathology Department of CHSJ.

Genomic DNA was extracted from FFPE tissues with the GRS Genomic DNA Kit – BroadRange (GRiSP, Portugal), according to the manufacturer's instructions.

The slides were deparaffinized in two consecutive incubations of 10 minutes in xylol, followed by two incubations of 5 minutes in ethanol 100%. After drying for 15 minutes at room temperature, the selected area was manually dissected from the slide and collected to a 1.5mL eppendorf tube. Buffer BR1 (200µL) and proteinase K (20µL; 20mg/µL) were added to each sample for disruption of cell membranes and protein digestion, and incubated overnight at 60°C with shaking (650 rpm). When necessary, additional 10µL of proteinase K were added for complete protein digestion. Buffer BR2 (200µL) was added to each sample and mixed by inversion several times. DNA precipitation was accomplished by adding pro-analysis ethanol 100% (200µL) and samples were vortexed for 10 seconds. The precipitated DNA was transferred to *gDNA plus spin columns* and centrifuged (Sorvall Legend Micro 21R centrifuge, Thermo Scientific, USA) at 16.000g for 1 minute at room temperature. The flow-through was discarded, and the spin columns were placed in new collection tubes. Two washing steps were performed: first, samples were washed with Wash Buffer 1 (400 µL) and centrifuged at 16.000g for 30 seconds at room temperature. After

discarding the flow-through, 600µL of Wash Buffer 2 were added and samples were centrifuged at 16.000g for 30 seconds at room temperature. The spin columns were dried with a final centrifugation at 16.000g for 3 minutes at room temperature. The spin columns were transferred to new eppendorf tubes (1.5mL) and 25 µL of preheated Elution Buffer were added to the column to elute the purified genomic DNA. Samples were incubated for 3 minutes at room temperature and centrifuged at 16.000g for 30 seconds. Additional 50 µL of preheated Elution Buffer were added for better output and a final centrifugation was performed at 16.000g for 1 minute.

DNA qualitative and quantitative analysis was performed using a NanoDrop (ND-1000, Thermo Fischer Scientific, Lithuania, EU) Spectrophotometer and samples were immediately stored at -20°C.

5. Genetic characterization

Tumor and adjacent tissue samples were analyzed for *FGFR3*, *RAS* (*NRAS*, *HRAS* and *KRAS*) and h*TERT* promoter mutations, described as the most frequent hotspot mutations in urothelial carcinomas.

5.1. Polymerase Chain Reaction (PCR)

The amplification of hotspot regions in *NRAS* (codon 61) was performed by standard Polymerase Chain Reaction (PCR), while *HRAS* (codons 12,13 and 61) and *KRAS* (codons 12, 13 and 61) hotspot mutations were analyzed by touchdown PCR. All PCR reactions were conducted using the Bioline PCR Kit (MyTaq HS Mix 2X, USA) in a thermal cycler system (SimpliAmp™ Thermalcycler, Applied Biosystems, USA), following the manufacturer's instructions (**Figure 6A** and **6B**). The mix composition and the specific primers (Forward and Reverse), optimized in the laboratory, used for each PCR reaction are represented in **Table 1** and **Table 2**, respectively.

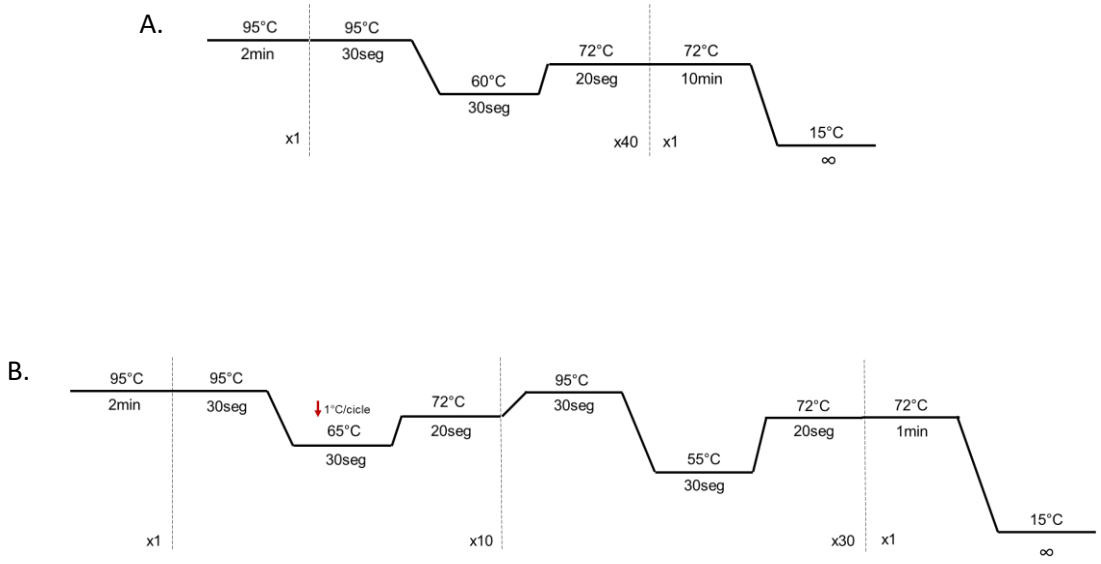

Figure 6. (A) Thermal cycler conditions applied in standard PCR for NRAS and (B) Thermal cycler conditions applied in touchdown PCR for HRAS and KRAS.

Table 1. Primers (Forward and Reverse) used in the PCR reactions for NRAS, HRAS and KRAS.

Gene	Primer sequences	Fragment size (bp)
NRAS	**F:** 5' - CAG AAA ACA AGT GGT TAT AGA TGG - 3' **R:** 5' - GTC CTC ATG TAT TGG TCT CTC A - 3'	102
HRAS1 (codons 12 and 13)	**F:** 5' - CAG GAG ACC CTG TAG GAG G - 3' **R:** 5' - TCG TCC ACA AAA TGG TTC TG - 3'	139
HRAS2 (codon 61)	**F:** 5' - GGA GAC GTG CCT GTT GGA - 3' **R:** 5' - GGT GGA TGT CCT CAA AAG AC - 3'	140
KRAS1 (codons 12 and 13)	**F:** 5' - GGC CTG CTG AAA ATG ACT G - 3' **R:** 5' - GGT CCT GCA CCA GTA ATA TG - 3'	163
KRAS2 (codon 61)	**F:** 5' - CCA GAC TGT GTT TCT CCC TT - 3' **R:** 5' - CAC AAA GAA AGC CCT CCC CA - 3'	155

Table 2. PCR mix composition for NRAS, HRAS and KRAS amplification.

Reagent	Quantity per sample
2x MyTaq HS Mix	5µL
Primer F	0.25µL
Primer R	0.25µL
H_2Od	3.5µL
DNA	-
Total	9µL

5.2. Electrophoresis and PCR product purification

To ensure PCR efficiency and evaluate DNA amplification, 1% agarose gel electrophoresis (GRS Agarose LE, GRiSP, Oporto, Portugal) was performed in 0.5x concentrated SGTB buffer (20x SGTB agarose electrophoresis buffer, GRiSP, Oporto, Portugal). A DNA ladder (Invitrogen, CA, USA) was added for molecular weight evaluation, and 2 µL of PCR product were mixed with 1µL of Loading Buffer dye containing Gel Red® Nucleic Acid Gel Stain 3X (Biotium, Inc., CA, USA). After each run, the agarose gel was exposed to UV light in the ChemiDocTM XRS+ System, from BIORAD (Universal Hood II, Hercules, CA, USA – 50/60 Hz) to verify amplification.

Purification of the amplified PCR products was conducted when no evidence of contamination was detected. ExoSAP is a combination of Exonuclease I (Thermo Scientific, Lithuania, EU) and Shrimp Alkaline Phosphatase (Thermo Scientifics, Lithuania, EU). After adding 1.5µL of ExoSAP to PCR products, two incubations were performed in a thermal cycler system (SimpliAmp™ Thermalcycler, Applied Biosystems, USA). The first incubation (30 minutes at 37ºC) is responsible for eliminating unwanted primers and dNTPs not processed during PCR reaction, while the second incubation (15 minutes at 85ºC) is necessary to inactivate both enzymes.

5.3. Sanger Sequencing

Hotspot mutations in amplified and purified PCR products were detected by Sanger Sequencing, using the BigDye® Terminator v3.1 Cycle Sequencing Kit (Applied Biosystems). The protocol was performed on ice and the sequencing products were amplified in a thermal cycler system (SimpliAmp™ Thermalcycler, Applied Biosystems, USA), following the manufacturer's instructions (**Figure 7**). The sequencing mix composition is described in **Table 3**.

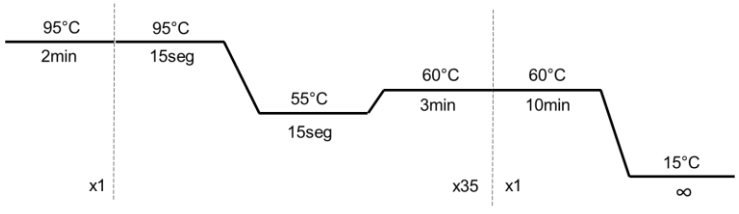

Figure 7. Thermal cycler conditions applied for Sanger Sequencing for NRAS, HRAS and KRAS.

Table 3. Sequencing mix composition for NRAS, HRAS and KRAS.

Reagent	Quantity per sample
BigDye	0.4µL
Sequencing Buffer	3.4µL
Primer	0.3µL
H_2Od	3.5µL
PCR product	-
Total	7.6µL

5.4. Sanger Sequencing Products Purification

The amplified sequencing products were purified using Sephadex™ G-50 resin fine columns (GE Healthcare Life Sciences, Little Chalfont, UK) to remove dNTPs and ddNTPs not incorporated in the DNA. Samples were transferred to the sequencing columns and centrifuged (Centrifuge 5417R, Eppendorf, Germany) at 3.200 rpm for 4 minutes at 4°C. After adding 15µL of HiDi™ Formamide (Applied Biosystems, Warrington, UK) to maintain the DNA in a denaturated state, samples were analyzed by capillary electrophoresis on Applied Biosystems 3500/3130XL Genetic Analyzers (California, USA). Detected mutations were confirmed and validated with an independent PCR and sequencing reactions.

5.5. Quantitative Real-Time PCR (qPCR)

Detection of target hotspot mutations in *TERT*p (c.1-124C>T and c.1-146C>T) and *FGFR3* (p.R248C and p.S249C) was performed by qPCR (QuantStudio™ 5 Real-Time PCR System, Applied Biosystems, USA), using specific primers and probes provided by the Uromonitor® test kit (U-monitor, Porto, Portugal) and performed according to the manufacturer's instructions (**Table 4A**, **4B**, **4C**, **4D** and **4E**).

Table 4. qPCR mix composition (A) for FGFR3 248 and 249 assays, (B) for FGFR3 negative control and (C) for TERTp -124 and -146 assays

(A)

Reagent	Quantity per well
Master mix	5µL
Primer 1	1µL
Primer 2	0.2µL
Probe 1	0.25µL
Probe 2	0.25µL
H_2Od	2.3µL
DNA	-
Total	9µL

(B)

Reagent	Quantity per well
Master mix	5µL
Primer 2	0.2µL
Probe 1	0.25µL
Probe 2	0.25µL
H_2Od	3.3µL
DNA	-
Total	9µL

Table 4. Continued.

(D)

Reagent	Quantity per well
Master mix	5µL
Primer 1	0.45µL
Primer 2	0.45µL
Probe 1	0.2µL
Probe 2	0.2µL
H_2Od	2.7µL
DNA	-
Total	9µL

For the mutational screening of *TERT*p (referred as *TERT* -124 and *TERT* -146), an allelic discrimination assay was performed using Locked Nucleic Acid (LNA) probes. These modified probes improve allelic discrimination by regulating the melting temperature of the probe and allowing it to bind with higher stability to the target DNA sequence.

For the mutational screening of *FGFR3* (referred as *FGFR3* 248 and *FGFR3* 249), a competitive allele-specific real-time PCR was performed. A molecular blocker suppresses amplification of the wild type allele by competing with the mutation allele-specific primer. Therefore, only the mutant allele is able to generate a fluorescent signal, increasing the specificity of the reaction.

A final volume of 9µL of qPCR mix were transferred into a 96-well PCR plate as well as approximately 25ng/µL of DNA per sample. Negative and positive controls were included in each run to validate the obtained results. Also, a non-template control (NTC) served to exclude the possibility of contamination. The PCR plates were sealed and loaded into the qPCR real-Time machine, following the predefined program specified in **Figure 8**.

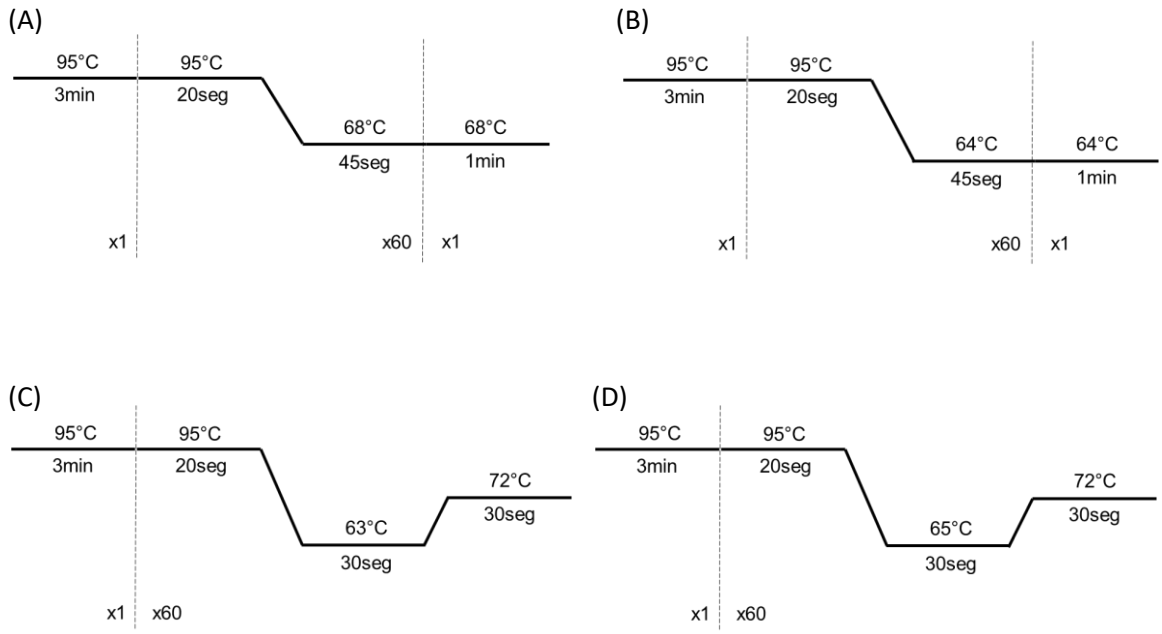

Figure 8. (A) Thermal cycler conditions applied for TERT -124 assay (B) Thermal cycler conditions applied for TERT -146 assay (C) Thermal cycler conditions applied for FGFR3 248 assay and (D) Thermal cycler conditions applied for FGFR3 249 assay and negative control.

6. Immunohistochemistry

CK5/6 and CK20 protein expression were evaluated with immunohistochemistry (IHC) staining procedures, performed on 3-µm FFPE tissue sections using UltraVision™ Quanto Detection System HRP (REF: TL-125-QHL, Thermo Scientific). Slides were deparaffinized twice in xylol (10 minutes each) and rehydrated in decreasing concentrations of ethanol for 5 minutes each (2x 100% ethanol, 96% ethanol and 70% ethanol). A single washing step was performed for 5 minutes in flowing water. Antigen retrieval was performed in a steamer at 90°C for 30 minutes in 10x concentrated Epitope Retrieval Solution (pH 9.0, REF. RE7119, Novocastra™, Leica Biosystems), followed by 20 minutes at room temperature. Slides were washed twice (for 5 minutes each) in 10% phosphate-buffered saline (PBS) and 0.02% tween washing buffer (referred as PBS-T 0.02%). After restricting the tissue area with a hydrophobic pen, endogenous peroxidase was blocked at room temperature (10 minutes each) with Ultravision™ hydrogen peroxide block (REF. TA-125-H202Q, Thermo scientific) and UltraVision™ protein block (REF. TA-125-PBQ, Thermo Scientific). Between incubations, two consecutive washes in PBS-T 0.02%, 5 minutes each, were performed. Slides were incubated with the primary antibodies specified in **Table 5**, diluted in antibody diluent OP Quanto (ready-to-use; REF. TA-125-ADQ, Thermo Scientific). Slides were left in a humid chamber at 4°C overnight for at least 16h and a maximum of 18h of incubation.

Table 5. Primary antibody experimental conditions used in immunohistochemical staining.

Primary Antibody	Vendor	Clone	Dilution
Monoclonal Mouse Anti-Human CK5/6	Dako (REF. M723701-2)	D5/16 B4	1:100
Monoclonal Mouse Anti-Human CK20	Dako (REF. M701901-2)	Ks20.8	1:100

After primary antibody incubation, slides were washed three times (5 minutes each) in PBS-T 0.02%, and the Primary Antibody Amplifier Quanto (REF. TL-125-QPB, Thermo Scientific) was added for 10 minutes at room temperature. Slides were washed twice in PBS-T 0.02%, followed by incubation with HRP Polymer Quanto (REF. TL-125-QPH, Thermo Scientific) for 10 minutes at room temperature. Regarding CK20, for chromogenic visualization, 3% diaminobenzidine chromogen (DAB, REF. TA-004-QHCX, Thermo Scientific) and DAB Quanto Substrate (REF. TA-125-QHSX, Thermo Scientific) were added and incubated for 3 minutes at room temperature. Regarding CK5/6, HIGHDEF® Red IHC Chromogen (HRP, REF. ADI-950-210-0030, Enzo Life Sciences) was added and incubated for 18 minutes at room temperature. Afterwards, slides were washed in flowing water for 5 minutes, counterstained with Gill's Hematoxylin Solution (Thermo Scientific) for 2 minutes and washed once again in flowing water (5 minutes) to remove the excess of stain. For CK20 immunostaining, extra steps were performed: slides were washed briefly in 0.02% (W/V) Ammonia water, followed by flowing water, and dehydrated with increasing concentrations of ethanol for 5 minutes each (96% ethanol and 100% ethanol). Slides were cleared in two 10-minute incubations in xylol and mounted with Richard–Allan Scientific™ Mounting Medium. CK5/6 slides were mounted with an aqueous mounting medium.

Positive (normal urothelium tissue for CK5/6 and appendix tissue for CK20) and negative (primary antibody omission) controls were included in each immunostaining procedure.

Semiquantitative expression analysis for both CK5/6 and CK20 was performed with a previously established scoring scheme, according to the intensity and proportion of positive-stained tumor cells. Staining intensity was evaluated as absent (0), faint (1), moderate (2) and strong (3), while the extent of positive-stained cells was scored as <5% (0), 5-25% (1), 25-50% (2), 50-75% (3) and >75% (4). The stablished score (from 0 to 7) resulted from the sum of the intensity and proportion of positive-stained tumors cells. Digitalization of CK5/6 slides was performed with the slide scanner NanoZoomer 2.0HT (Hamamatsu Photonics), by the Slides Digitalization Service of IPATIMUP.

7. Statistical Analysis

All statistical analysis was performed using the IBM SPSS® Software Version 27.0 (IBM, New York, USA). Univariate analysis was performed resorting to the Chi-square test or, when adequate, Fisher's exact test (Yates correction for data with multiple entries). Student's unpaired *t*-test was also conducted for independent samples (One-way ANOVA for multiple entries) or the Wilcoxon signed-rank test if the data was not normally distributed. Multivariate binary logistic regression was performed to evaluate the effect of the clinicopathological features and mutational profile of the tumor on the development of distant metastases. Differences were considered statistically significant when p-value<0.05.

Results

1. Clinicopathological and demographic data

A database was elaborated for the analysis and characterization of the patients' clinicopathological data, gathered from the information available in clinical and histological reports at CHUSJ. The molecular data obtained during this study was added to the database for further statistical analysis.

This series included 114 patients and respective 141 samples of upper urinary tract urothelial carcinoma. A total of 125 tumors (88.6%), 8 associated epithelial lesions (CIS) (5.7%) and 8 LN metastases (5.7%) were studied. Only the primary lesions were evaluated for statistical analysis, while LN metastases as well as CIS samples were excluded and analyzed separately.

Several parameters were evaluated, related to patients' demographic and clinical characteristics such as age and gender as well as the pathological features of the tumors (**Table 6**) and follow-up data (**Table 7**).

From the 114 patients, 33 (28.9%) were female, with a mean age of 80.5 ± 1.9 years, ranging from 53 to 99 years of age. A prevalence of male patients was found in this series (81/114, 71.1%) with a mean age of 76.6 ± 1.2 years, ranging from 44 to 99 years of age. The mean age of patients was of 77.7 ± 10.9, ranging from 44 to 99 years of age (**Table 6**).

Most of the individuals presented tumors in the renal pelvis (60.5%) while 27.2% of tumors occurred either at the proximal, middle, distal or pelvic portion of the ureter. Multiple tumors were found in both renal pelvis and various portions of the ureter in 14 patients (12.3%) (**Table 6**).

Regarding tumor laterality, a slight predominance of the right side was observed in 52.6% of all tumors in comparison to 54 (47.4%) tumors on the left side. Other histopathological characteristics were evaluated such as the presence of associated epithelial lesions. Most patients did not present these lesions (80.4%) but 19 (17.0%) showed tumors with associated CIS, two presented dysplasia (1.8%) and another presented both CIS and dysplasia (0,9%). The majority of cases did not show lymphatic invasion (70%), nor venous invasion (72.7%) (**Table 6**).

Table 6. Patient's age and gender and clinicopathologic characteristics of all tumors.

Clinicopathological characteristics	All tumors (N=114)
Age, mean ± SD (n=114)	77.72 ± 10.93
Gender (n=114)	
Female	33 (28.9%)
Male	81 (71.1%)
Tumor location (n=114)	
Renal pelvis	69 (60.5%)
Ureter	31 (27.2%)
Multiple	14 (12.3%)
Tumor side (n=114)	
Right	60 (52.6%)
Left	54 (47.4%)
Epithelial associated lesions (n=112)*	
Absent	90 (80.4%)
Present	22 (19.6%)
Lymphatic invasion (n=110)*	
Absent	77 (70%)
Present	33 (30%)
Venous invasion (n=110)*	
Absent	80 (72.7%)
Present	30 (27.3%)

*Total cases lower than 114 due to lack of information in some parameters

At diagnosis, high grade tumors were found in a striking number of cases (105/112; 93.8%) while low grades tumors represented 6.3% of primary tumors. The majority of patients were at T3 stage (46%), while 7 (6.3%) were at Ta or Tis stage, 27 (24.3%) at T1 stage, 19 (17.1%) at T2 stage and 7 (6.3%) at T4 stage.

Additionally, 8 out of 109 patients presented LN metastasis (7.3%); however, in the majority of the patients, lymph nodes were not assessed (Nx = 70.6%). Distant metastasis

was present in 13 primary samples, corresponding to 13.5% of all tumors. In most patients (79/96; 82.3%), no metastasis was identified (**Table 7**).

Regarding clinical management and follow-up, 105 patients (92.1%) were submitted to nephroureterectomy. Other surgical procedures were performed, such as partial ureterectomy and nephroscopy with resection, corresponding to a minority of 6.1% and 1.8% of cases, respectively. Surgical margins were inspected after treatment and the absence of residual tumor was found in 96 (87.3%) of the cases, while 10 patients (9.1%) presented microscopical residual tumor and 4 (3.6%) presented macroscopic residual tumor (**Table 7**).

Table 7. Patient's staging and treatment characteristics data of all tumors.

Clinical follow-up	All tumors (N=114)
Tumor grade (n=112)*	
Low	7 (6.3%)
High	105 (93.8%)
Staging T (n=111)*	
Ta / Tis	7 (6.3%)
T1	27 (24.3%)
T2	19 (17.1%)
T3	51 (46%)
T4	7 (6.3%)
Staging N (n=109)*	
N0	24 (22%)
N1	6 (5.5%)
N2	2 (1.8%)
Nx	77 (70.6%)
Staging M (n=96)*	
M0	79 (82.3%)
M1	13 (13.5%)
Mx	4 (4.2%)

*Total cases lower than 114 due to lack of information in some parameters.

(Continued)

Table 7 – Continued.

Clinical follow-up	All tumors (N=114)
Treatment procedure (n=114)	
Nephroureterectomy	105 (92.1%)
Partial ureterectomy	7 (6.1%)
Nephroscopy with resection	2 (1.8%)
Residual tumor (n=110)*	
R0	96 (87.3%)
R1	10 (9.1%)
R2	4 (3.6%)

*Total cases lower than 114 due to lack of information in some parameters.

Some statistically significant and borderline associations were found between the clinicopathological features mentioned above (**Supplementary Table I**). It is of note that some variables, such as treatment procedure, presented very few cases on some categories (for example, partial ureterectomy and nephroscopy with resection). Therefore, the obtained results must be taken with caution.

Of relevance, it was observed that patients with venous invasion had a higher mean age (81.6 ± 9.1 vs 76,7 ± 11.3 ; p=0.037). Older age also correlated with the presence of residual tumor (p=0.004). Specifically, patients with R2 had a higher mean age (91,5 ± 9,5) than R0 patients (76.5 ± 10.8). Also, absence of epithelial associated lesions was associated with absence of venous invasion (p=0.049) and lymphatic invasion (p=0.031). Regarding treatment procedure, more than 95% of patients with a renal pelvis tumor were submitted to nephroureterectomy while all patients that were submitted to partial ureterectomy presented a ureteric tumor. Treatment procedure (i.e. nephroureterectomy) also correlated with tumors of higher grade (p<0.001). Additionally, patients with LN metastasis were all submitted to a more invasive procedure, nephroureterectomy (p=0.001) (**Supplementary Table I**).

As expected, presence of lymphatic invasion was associated with presence of venous invasion (p<0.001) and higher T stages (p<0.001). Additionally, most patients with distant metastasis presented lymphatic (p=0.006) and venous invasions (p<0.001). Presence of venous invasion was also more frequent in patients with higher T stages (p<0.001). Patients with residual tumors (R1 or R2) were also associated with presence of venous invasion (p=0.004). Regarding tumor grade, patients with higher T stages (T2, T3 and T4) presented

high grade tumors (p<0.001). Distant metastasis was also more frequent in higher T stages such as T3 and T4 (p=0.002). When no distant metastasis was present, most patients didn't present residual tumors (p=0.037) (**Supplementary Table I**).

2. Genetic characterization of UTUC samples

The molecular status for TERTp, FGFR3, and RAS (NRAS, HRAS and KRAS) genes was evaluated and summarized in **Table 8**. Representative images of mutations found in each studied gene are represented in **Supplementary Figures II-VI**.

Table 8. Patient's mutational status for all tumors.

Genes	n	WT	Mutated	Mutation type
TERTp	131*	60 (45.8%)	71 (54.2%)	53 (-124 C>T) 18 (-146 C>T)
FGFR3	137*	61 (44.5%)	76 (55.5%)	47 (p.R248C) 21 (p.S249C) 8 (p.R248C, p.S249C)
NRAS	141	140 (99.3%)	1 (0.7%)	1 (p.Q61R)
HRAS	141	138 (97.9%)	3 (2.1%)	1 (p.G12D) 1 (p.G13R) 1 (p.Q61R)
KRAS	140*	131 (93.6%)	9 (6.4%)	1 (p.V14I) 1 (p.Q61P) 2 (p.G12A) 5 (p.G12D)

*Total number of cases lower than 141 due to technical issues

Out of 141 UTUC samples, 106 (75,2%) were mutated for at least one of the studied genes. Specifically, 71 samples (54.2%) were found mutated for TERTp, 76 (55.5%) for FGFR3, nine (6.4%) for KRAS, three (2.1%) for HRAS and one (0.7%) for NRAS (**Table 8**).

Regarding TERTp mutations, two mutational hotspots were detected (-124 C>T and -146 C>T). The majority of mutations occurred at the -124 C>T hotspot, corresponding to 74.6% (53/71) of TERTp mutations. Out of 76 FGFR3 mutated samples, 47 (61.8%) were found at the p.R248C hotspot, 21 (27.6%) were found at the p.S249C hotspot and 8 presented both FGFR3 mutations. Only one mutation was found in NRAS (p.Q61R), corresponding to less than 1% of tumors. Concerning HRAS, three alterations were found

in codons 12, 13 and 61 (p.G12D, p.G13R and p.Q61R), corresponding to 2.1% of tumors. The most common mutated Ras gene was KRAS (6.4% of all tumors) with one alteration found in p.V14I, one in p.Q61P, 2 in p.G12A and 5 in p.G12D (**Table 8**). Overall, 12 cases (8.5% of all tumors) presented RAS mutations and 1 case presented simultaneous RAS alterations (HRAS at hotspot p.G13R and KRAS at hotspot p.Q61P) (data not shown).

Other concomitant molecular alterations were found between the studied genes. From all tumors, 46 showed double mutation for TERTp and FGFR3 (**Supplementary Table II**). This association was statistically significant (p=0.018) which is in concordance with the literature since these mutations frequently co-occur in the same tumor [94]. Additionally, 6 tumors presented a TERTp mutation as well as a RAS mutation (**Supplementary Table III**). Interestingly, 6 tumors were also simultaneously mutated for both FGFR3 and RAS genes (**Supplementary Table IV**).

Of note, one sample presented TERT -124 C>T, FGFR3 p.S249C and HRAS p.G12D; one sample presented TERT -146 C>T, FGFR3 p.R248C and KRAS p.V14I; one sample presented TERT -146 C>T, FGFR3 p.R248C, HRAS p.G13R and KRAS p.Q61P; and another two samples (same case) presented TERT -124 C>T, FGFR3 p.R248C and KRAS p.G12D. No overlapping mutations were found between NRAS and other genes (**Table 9**).

Table 9. UTUC tumors with more than two concomitant mutations.

Case	Age	Gender	Lesion	Genes	Genetic alterations
29	76	Female	Primary tumor	*TERT*p, *FGFR*3 and *HRAS*	-124 C>T, p.S249C and p.G12D
74	60	Female	Primary tumor	*TERT*p, *FGFR*3 and *KRAS*	-146 C>T, p.R248C and p.V14I
107	83	Male	Primary tumor	*TERT*p, *FGFR*3, *HRAS* and *KRAS*	-146C>T, p.R248C, p.G13R and p.Q61P
108	84	Male	Primary tumor	*TERT*p, *FGFR*3 and *KRAS*	-124 C>T, p.R248C and p.G12D
			LN metastasis	*TERT*p, *FGFR*3 and *KRAS*	-124 C>T, p.R248C and p.G12D

2.1. Genetic alterations in carcinoma *in situ* samples

In this series, 8 epithelial associated lesions, specifically carcinomas *in situ* (CIS), were concomitant with another primary lesion. Of those, only three were found mutated (one sample (25.0%) for TERTp and two samples (40.0%) for FGFR3) and no concomitant

alterations were observed (**Supplementary Table V**). These lesions were mainly present in male patients of older age (70-95 years old) (**Table 10**).

Compared with the other primary lesion present in the same patient, the CIS lesion presented distinct mutational profiles in two cases (**Table 10**). In case 29, only the primary tumor presented alterations at -124 C>T hotspot (TERTp) and at p.G12D hotspot (HRAS), and, in case 40, only the carcinoma *in situ* sample presented an alteration at the -124 C>T hotspot (**Table 10**).

Table 10. Molecular profile of the primary tumors and the corresponding CIS.

Case	Age	Gender	Lesion	TERTp	FGFR3	RAS
9	95	Male	Primary tumor	WT	WT	WT
			CIS	WT	WT	WT
13	76	Male	Primary tumor	-146 C>T	p.R248C	WT
			CIS	-	-	WT
21	70	Male	Primary tumor	WT	WT	WT
			CIS	WT	WT	WT
29	76	Female	Primary tumor	-124 C>T	p.S249C	p.G12D (HRAS)
			CIS	WT	p.S249C	WT
36	75	Male	Primary tumor	WT	**p.R248C**	WT
			CIS	-	-	WT
40	78	Female	Primary tumor	WT	WT	WT
			CIS	**-124 C>T**	WT	WT
41	84	Male	Primary tumor	WT	-	WT
			CIS	-	-	WT
62	89	Male	Primary tumor	-124 C>T	p.R248C	WT
			CIS	-	p.R248C	WT

2.2. Genetic alterations in lymph node metastases

From 141 samples, 8 LN metastases were studied for genetic characterization. These lesions were mainly present in male patients of older age (76-89 years old) (**Table 12**).

From the 8 LN metastasis studied, five (62.5%) were found mutated for FGFR3, four (57.1%) were TERTp mutated (mainly at the -124 C>T hotspot) and two (25.0%) presented KRAS mutations (p.G12A and p.G12D) (**Table 11**).

Table 11. Genetic alterations in lymph node metastases.

Genes	n	WT	Mutated	Mutation type
***TERT*p**	7*	3 (42.9%)	4 (57.1%)	3 (-124 C>T) 1 (-146 C>T)
***FGFR*3**	8	3 (37.5%)	5 (62.5%)	4 (p.R248C) 1 (p.R248C, p.S249C)
NRAS	8	8 (100%)	0 (0%)	-
HRAS	8	8 (100%)	0 (0%)	-
KRAS	8	6 (75.0%)	2 (25.0%)	1 (p.G12A) 1 (p.G12D)

*Total number of cases lower than 9 due to technical issues

Only one LN metastasis was considered wild-type for all genes while the remaining 7 (87.5%) presented at least one of the studied mutations. Of those 7 LNM samples, 3 presented concomitant mutations: one with TERT -146 C>T and FGFR3 p.R248C, one with TERT -124 C>T and both FGFR3 mutations (p.R248C and p.S249C) and another with TERT -124 C>T, FGFR3 p.R248C and KRAS p.G12D (**Table 12**).

From the 8 LN metastases studied in this series, 2 presented a distinct mutational profile compared to its corresponding primary tumor (**Table 12**). While the primary tumors were considered wild-type for all genes, the LN metastases presented an extra alteration either in the TERTp -124 C>T hotspot or in FGFR3 p.R248C hotspot.

Table 12. Molecular profile of the primary tumors and the corresponding LN metastases.

Case	Age	Gender	Lesion	TERTp	FGFR3	RAS
4	89	Male	Primary tumor	WT	WT	p.G12A (KRAS)
			LNM	WT	WT	p.G12A (KRAS)
13	76	Male	Primary tumor	-146 C>T	p.R248C	WT
			LNM	-146 C>T	p.R248C	WT
28	78	Male	Primary tumor	WT	WT	WT
			LNM	**-124 C>T**	WT	WT
33	82	Female	Primary tumor	-	p.R248C	WT
			LNM	-	p.R248C	WT
40	78	Female	Primary tumor	WT	WT	WT
			LNM	WT	WT	WT

(Continued)

Table 12 – Continued.

Case	Age	Gender	Lesion	TERTp	FGFR3	RAS
69	82	Male	Primary tumor	WT	WT	WT
			LNM	WT	**p.R248C**	WT
83	82	Female	Primary tumor	-124 C>T	p.R248C, p.S249C	WT
			LNM	-124 C>T	p.R248C, p.S249C	WT
108	84	Male	Primary tumor	-124 C>T	p.R248C	p.G12D (KRAS)
			LNM	-124 C>T	p.R248C	p.G12D (KRAS)

Due to the reduce number of lesions of CIS and LN metastases in this series, only the primary tumors were selected for the subsequent statistical analysis (section **3.**).

3. Relationship between molecular alterations and clinicopathological features in primary tumors

Since some patients presented more than one tumor sample, only the sample that presented genetic alterations was considered for statistical analysis.

Out of 114 UTUC patients, 89 (78.1%) presented tumors mutated for at least one of the studied genes (data not shown). TERTp was found mutated in 63 cases (57.3%), mainly at the -124 C>T hotspot, while 62 cases (54.9%) presented FGFR3 mutated tumors with a predominance of the p.R248C alteration. Only one case (<1%) presented a NRAS mutated tumor, 4 cases (3.5%) harbored HRAS alterations (found at codons 12, 13 and 61) and 7 cases (6.2%) were found mutated for KRAS, mainly at codon 12 (**Table 13**). Overall, 11 cases (9.6% of primary tumors) presented tumors with RAS mutations and 1 case presented concomitant RAS alterations (HRAS at hotspot p.G13R and KRAS at hotspot p.Q61P) (data not shown).

Table 13. Patient's mutational status in primary tumors.

Genes	n =	WT	Mutated	Mutation type
***TERT*p**	110*	47 (42.7%)	63 (57.3%)	46 (-124 C>T) 16 (-146 C>T)
***FGFR*3**	113*	51 (45.1%)	62 (54.9%)	38 (p.R248C) 9 (p.S249C) 5 (p.R248C, p.S249C)
NRAS	114	113 (99.1%)	1 (0.9%)	1 (p.Q61R)
HRAS	114	110 (96.5%)	4 (3.5%)	1 (p.G12D) 1 (p.G13R) 1 (p.Q61R)
KRAS	113*	106 (93.8%)	7 (6.2%)	1 (p.V14I) 1 (p.Q61P) 1 (p.G12A) 4 (p.G12D)

*Total number of cases lower than 114 due to technical issues

To correlate genetic alterations in TERTp, FGFR3, NRAS, HRAS and KRAS genes with the available clinicopathological features and follow-up data of the patients and tumors, univariate analysis was performed and described in **Supplementary Tables VI-VIII**. Description of borderline variables ($p<0.10$) as well as the statistically significant (p-value <0.05) associations found in this series is presented below. Patient's age and gender are always present, regardless of statistical significance. For statistical analysis, "Staging N" and "Staging M" variables were grouped into the following categories: Nx/N0, N1 and N2; and Mx/M0 and M1, respectively.

Several associations were analyzed between the mutation status of TERTp and the clinicopathological and follow-up data of the patients (**Supplementary Table VI**). However, no statistically significant or informative associations were found in this series.

*FGFR*3 mutations were analyzed for the clinicopathological characteristics mentioned previously (**Supplementary Table VII**). Of relevance, the presence of these mutations was more frequent in cases without lymphatic ($p=0.003$) nor venous invasions ($p= 0.001$).

Table 14. Univariate analysis for FGFR3 mutations status and clinicopathological characteristics of primary tumors.

Parameters	*FGFR3*		p-value
	WT	Mutated	
Clinicopathological features			
Age, mean ± SD (n=113)	77.88 ± 10,53	77.48 ± 11,39	0.848
Gender (n=113)			
Female	14 (27.5%)	19 (30.6%)	0.710
Male	37 (72.5%)	43 (69.4%)	
Lymphatic invasion (n=109)*			
Absent	27 (55.1%)	49 (81.7%)	**0.003**
Present	22 (44.9%)	11 (18.3%)	
Venous invasion (n=109)*			
Absent	28 (57.1%)	51 (85.9%)	**0.001**
Present	21 (42.9%)	9 (15.0%)	

* Total number of cases lower than 113 due to missing clinical information

No relevant or statistically significant associations were established between the overall presence of RAS mutations and clinicopathological characteristics (**Supplementary Table VIII**). It was observed an association between NRAS mutations and younger patients (p=0.036) as well as absence of LN metastasis (p<0.001). However, since only one NRAS mutation was found in this series, these results should be taken with caution. Additionally, a borderline association was observed between absence of KRAS mutations and absence of LN metastasis (p=0.096) (**Table 15**).

Table 15. Statistically significant associations between NRAS and KRAS mutations and clinicopathological characteristics of primary tumors.

Genes	Parameters	WT	Mutated	p-value
NRAS	**Clinicopathological features**			
	Age, mean ± SD (n=114)	77.92 ± 10.76	55	**0.036**
	Gender (n=114)			
	Female	33 (29.2%)	0 (0%)	0.521
	Male	80 (70.8%)	1 (100%)	
	Staging N (n=109)*			
	N0/Nx	100 (92.6%)	1 (100%)	
	N1	6 (5.5%)	0 (0%)	**<0.001**
	N2	2 (1.9%)	0 (0%)	
KRAS	**Clinicopathological features**			
	Age, mean ± SD (n=113)*	77.33 ± 10.829	82.71 ± 12.593	0.210
	Gender (n=113)*			
	Male	74 (69.8%)	6 (85.7%)	0.370
	Female	32 (30.2%)	1 (14.3%)	
	Staging N (n=104)*			
	N0/Nx	95 (94.1%)	5 (71.4%)	
	N1	4 (4.0%)	2 (28.6%)	0.096
	N2	2 (2.0%)	0 (0%)	

* Total number of cases lower than 114 due to missing clinical information

4. Predictive model of metastasis

Finally, we sought to evaluate the impact of molecular alterations and other clinicopathological features as predictive factors in the development of metastasis.

In previous sections, we determined statistically significant associations between molecular alterations and clinicopathological features using univariate analyses. Regarding distant metastasis (stage M), we found an association with the presence of lymphatic ($p=0.006$) and with venous ($p<0.001$) invasion, residual tumor ($p=0.037$) and with higher staging T ($p=0.002$).

These factors, that supposedly influenced the output (distant metastasis), were used to conduct a multivariate analysis and, ultimately, adjust and eliminate variables that could be influencing our results.

A binary logistic regression model was chosen to include both clinical and molecular variables that were deemed significant with univariate analyses such as lymphatic invasion, venous invasion and residual tumor. Other factors such as age (as a continuous variable) and gender were always included for proper adjustment and the output evaluated was distant metastasis. Although not statistically significant, genetic mutations were considered for the model to understand if they could influence the development of metastasis.

After adjusting all statistically significant variables and all studied genes, only the clinicopathological variables remained significant (data not shown). Staging T was not possible to evaluate since it resulted in a confounding effect and wasn't added to the final model. When only creating a model for the genetic alterations (and age and gender), none were significant; therefore, were removed from further analysis.

The final model is represented in **Table 16**. Only venous invasion remained a predictive factor for the development of distant metastases when testing for all variables, including gender and age. It was observed that patients with tumors presenting venous invasion were 8.9 times more likely to develop distant metastases than patients with tumors without evidence of venous invasion.

Of note, when removing vascular invasion from the multivariate model, residual tumor remained significant as expected (data not shown).

Table 16. Clinicopathological features as predictors of distant metastases.

		Univariate analysis		**Multivariate analysis**	
Parameters	**Stage M** (n=95)	**OR (95% CI)**	**p-value**	**OR (95% CI)**	**p-value**
Age	-	1.04 (0.98-1.10)	0.248	-	
Gender					
Female	30 (31.6%)	1 (reference)	0.529	-	
Male	65 (68.4%)	0.68 (0.20-2.28)			
Lymphatic invasion					
Absent	67 (70.5%)	1		-	
Present	28 (29.5%)	0.20 (0.06-0.69)	**0.010**		

(Continued)

Table 16 - Continued.

		Univariate analysis		Multivariate analysis	
Parameters	**Stage M** (n=95)	**OR (95% CI)**	**p-value**	**OR (95% CI)**	**p-value**
Venous invasion					
Absent	70 (73.7%)	1	**0.001**	8.9 (2.36-33.95)	**0.001**
Present	25 (26.3%)	9.3 (2.53-34.00)			
Residual Tumor					
R0	84 (88.4%)	1			
R1	8 (8.4%)	5.9 (1.17-29.14)	**0.031**	-	
R2	3 (3.2%)	19.5 (1.59-239.54)	**0.020**		

5. CK5/6 and CK20 immunohistochemistry in UTUC tumors

Immunohistochemistry was performed in a series of 141 UTUC samples. Distinct patterns of expression were observed within the analyzed samples, ranging from a high percentage of positive cells to a high percentage of negative cells for either CK5/6 (red staining) or CK20 (brown staining), as represented in **Figure 9** and **Figure 10**, respectively. Most cases presented a cytoplasmic immunostaining, while a few also presented membrane-specific protein expression. No nuclear staining was observed.

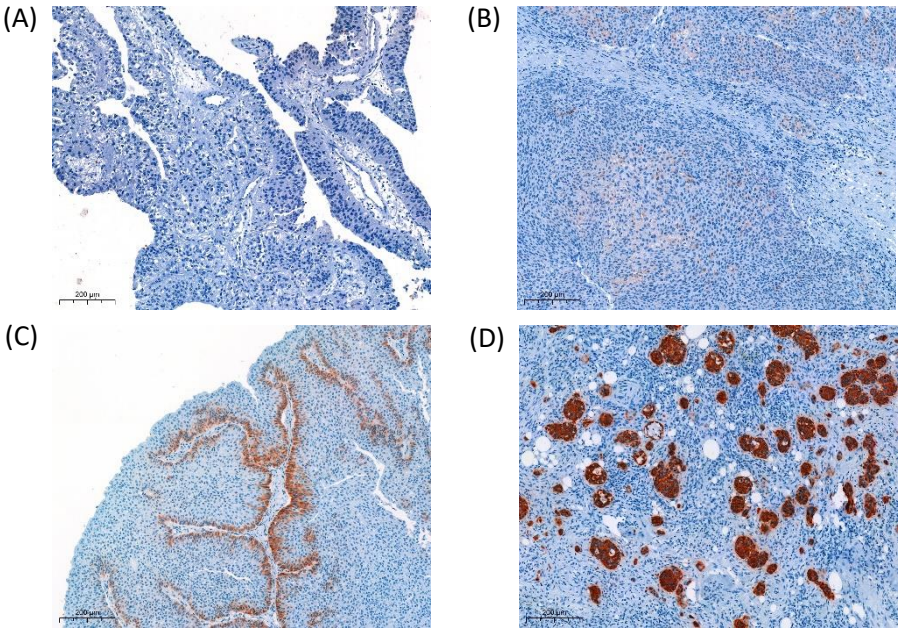

Figure 9. Intensity of CK5/6 expression: (A) absent protein expression; (B) faint protein expression; (C) moderate protein expression; and (D) strong protein expression (scale bar of 200µm).

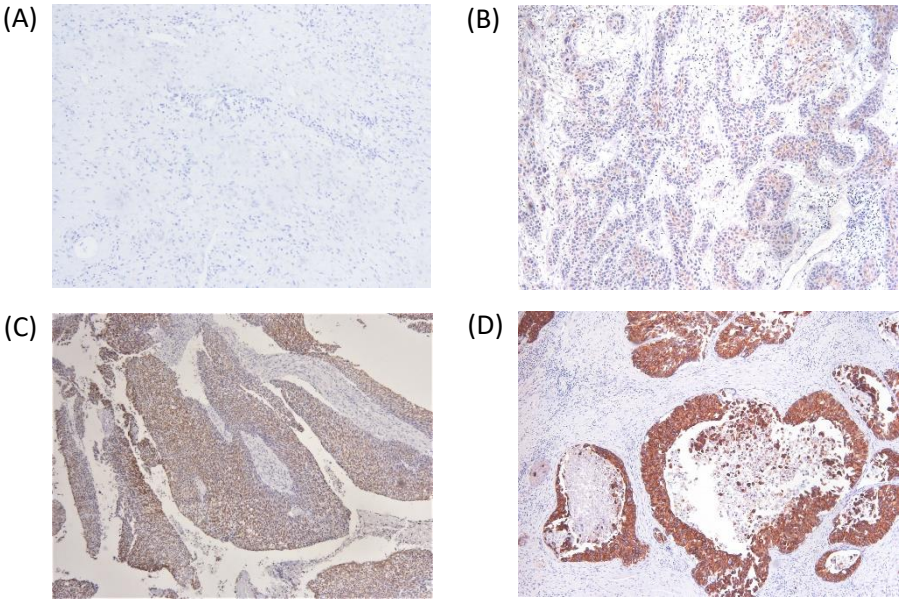

Figure 10. Intensity of CK20 expression: (A) absent protein expression; (B) faint protein expression; (C) moderate protein expression; and (D) strong protein expression (100x magnification).

CK5/6 staining in normal tissue is specific to the basal/intermediate layer, while CK20 presents a superficial luminal-specific expression (**Supplementary Figure VI**). However, in most tumors, we observed an aberrant type of expression, extended beyond the designated layers.

The results regarding the scoring scheme for cytokeratins 5/6 and 20 are summarized in **Table 17** and **Table 18**, respectively. Most lesions presented a score of 3 or 4, either for CK5/6 (30.5% and 36.9%, respectively) or CK20 (19.9% and 26.2%, respectively). No maximum score was obtained for CK5/6, while 8 tumors were given score 7 for CK20. Additionally, 6 tumors were considered negative (0) for CK5/6 and 20 tumors for CK20 expression.

Table 17. Scoring system performed for CK5/6 antibody.

	Score (CK5/6)							
	0	**1**	**2**	**3**	**4**	**5**	**6**	**7**
Frequency (%)	6 (4.3%)	3 (2.1%)	7 (5.0%)	43 (30.5%)	52 (36.9%)	23 (16.3%)	7 (5.0%)	0 (0%)

Table 18. Scoring system performed for CK20 antibody.

	Score (CK20)							
	0	**1**	**2**	**3**	**4**	**5**	**6**	**7**
Frequency (%)	20 (14.2%)	2 (1.4%)	11 (7.8%)	28 (19.9%)	37 (26.2%)	17 (12.1%)	18 (12.8%)	8 (5.7%)

Histological grades were compared regarding their CK5/6 and CK20 immunostaining (**Table 19** and **Table 20**). Regarding CK5/6, low grade tumors were mainly scored 3 (37.5%), while high grades tumors presented a more dispersed expression pattern, ranging from a score 0 to a score 6. For CK20, a score of 6 was the maximum score obtained in low grade tumors and the majority presented a score of 5. High grade tumors were once again classified within a high range of scores (from 0 to 7), specifically all the 20 tumors considered negative for CK20 expression were high grade as well as the 8 tumors presenting the highest classification score (**Table 20**).

Table 19. Comparison of the scoring system for CK5/6 between histological grades.

	Score (CK5/6)							
	0	**1**	**2**	**3**	**4**	**5**	**6**	**7**
Low grade*	0 (0%)	0 (0%)	0 (0%)	4 (50.0%)	1 (12.5%)	3 (37.5%)	0 (0%)	0 (0%)
High grade*	6 (4.6%)	3 (2.3%)	7 (5.3%)	39 (29.8%)	50 (38.2%)	19 (14.5%)	7 (5.3%)	0 (0%)

* Total number of cases lower than 141 due to missing clinical information

Table 20. Comparison of the scoring system for CK20 between histological grades.

	Score (CK20)							
	0	**1**	**2**	**3**	**4**	**5**	**6**	**7**
Low grade*	0 (0%)	0 (0%)	0 (0%)	2 (25.0%)	3 (37.5%)	2 (25.0%)	1 (12.5%)	0 (0%)
High grade*	20 (15.3%)	2 (1.5%)	9 (6.9%)	26 (19.8%)	34 (26.0%)	15 (11.4%)	17 (13.0%)	8 (6.1%)

* Total number of cases lower than 141 due to missing clinical information

No statistical analysis comparing clinicopathological data and immunohistochemistry was performed as this is still a preliminary analysis that requires a more comprehensive analysis of the slides.

Discussion

Upper urinary tract urothelial carcinoma is a relatively rare and aggressive disease with a higher incidence in developed countries. Several clinical and pathological factors affect the development and progression of UTUC, leading to recurrences and poor prognosis [21, 23, 26, 27, 34, 35]. The ability to diagnose and treat patients more efficiently could arise from a better understanding of the genetic background of this cancer and, ultimately, improve prognosis and therapy without submitting patients to highly invasive procedures.

Our main aim was to establish the status of the most common genes altered in UTUC (TERTp, FGFR3 and RAS genes) and understand their impact in the development and progression of the disease.

Our study was composed of 114 UTUC patients and their corresponding 141 samples from which 125 (88.6%) tumors, 8 (5.7%) CIS and 8 (5.7%) LN metastases were evaluated. These patients were followed and submitted to a surgical procedure in CHUSJ, between the years of 2009 and 2019, inclusive. As expected, our series was mainly composed of male patients (71.1%) between the ages of 53 to 99 years old. Moreover, an incidence ratio of 2.5 (male/female) was observed, confirming the gender disparity reported in the literature (male patients have an incidence of UTUC up to three times higher than female patients) [21, 30, 31].

Most of the individuals presented pelvicalyceal tumors while the remaining patients either presented tumors in the ureter or in multiple sites. The literature states that UTUC arising from the renal pelvis is twice more common than ureteric tumors and we also observed a similar ratio [21, 29, 39]. We observed more tumors of the right side of the tissue, but similar to other articles this clinicopathological variable wasn’t significant [25, 51].

Interestingly, our series was composed of tumors with more aggressive behavior, as described next. High-grade tumors composed almost all the cases of our series and only 7 were considered low-grade. Similarly, the majority of tumors were at T3 stage. Of note, a high number of patients presented high-grade invasive disease at diagnosis, which is in accordance with the current literature regarding its aggressive biology [21, 23, 34, 35].

From 114 patients, 105 were submitted to nephroureterectomy which is a highly invasive procedure that removes the kidney, ureter and a small part of the bladder where it connects with the ureter. Since most of the patients presented high-grade and invasive disease, this surgery is the most adequate to try and prevent tumor dissemination and progression [45]. Therefore, patients with less aggressive disease were submitted to other treatment procedures, such as partial ureterectomy and nephroscopy with resection, to preserve most

of the organs. As expected, treatment procedure (i.e. nephroureterectomy) correlated with tumors of higher grade and was performed in most patients with LN metastasis.

Other clinicopathological characteristics of the tumors were assessed and some associations were established. It is important to note that some variables, such as the treatment procedure and histological grade, presented wide differences or low number of effectives in some categories. So, the associations found with other clinicopathological characteristics should be taken with caution.

Langner *et al.* [63] described associations between the presence of vascular invasion, high pT classification and high-grade tumors. Of relevance, we also observed that patients with venous invasion had a higher mean age and presented tumors with a higher T stage. Therefore, venous invasion seems to be related with more aggressive cancer features and factors of poor prognosis. In future analyzes, it would be interesting to correlate this variable with disease outcome.

Patients with residual tumors were also associated with presence of venous invasion and older age. Similar results were obtained for lymphatic invasion, which was associated with presence of venous invasion and higher T stages. Distant metastasis correlated with lymphatic, venous invasions and higher T stages.

In our series, the majority of the tumors presented at least one of the studied mutations (*TERT*p, *FGFR*3 and/or *RAS*) and, as expected, *FGFR*3 alterations represented the major mutational event with similar results to others previously reported [95, 118, 119]. TERTp was mutated in 54% of the samples, followed by RAS genes mutations observed in 8.5% of all tumors. TERTp mutation frequencies are similar to what has been described by Killela *et al.* [100] regarding upper urinary tract tumors (47.3%). Vinagre *et al.* [106] also reported TERTp mutations with a frequency of 59% but in bladder carcinoma.

In concordance with the literature [94, 103], we verified that the majority of TERTp mutations occurred at the -124 C>T hotspot. Regarding FGFR3 hotspot mutations and according to the current literature [76, 93, 95], mutations at codon 249 are the most prevalent. Interestingly, we identified a higher prevalence of mutations at the p.R248C hotspot. Since we used qPCR, a highly sensitive technique, there is a higher probability to detect these alterations, previously missed by other laboratory procedures such as Sanger sequencing. In this case, we can hypothesize that due to UTUC heterogeneity, clones with an FGFR3 alteration at codon 248 could represent a smaller representation in the tumor and, in reality, the frequency of p.R248C mutations in urothelial cancer might be higher than currently reported.

NRAS mutations were fairly rare in this cohort, representing less than 1% of tumors. This mutation was found in a single case at codon 61 (p.Q61R) which is reported as the most prominent hotspot mutation in this gene [86, 90, 96]. Concerning HRAS, one mutation was found for each one of the most affected codons (12, 13 and 61) in human cancer. KRAS, p.G12D was the most common represented mutation, as reported in the literature [90, 96].

We found, however, discrepancies for the mutation frequency of certain RAS hotspot regions. Overall, we found 2.1% of HRAS gene mutated tumors but in different cohorts the prevalence is higher. For example, Audenet *et al.* reported an HRAS mutational frequency of 12% in UTUC. We cannot exclude that the small sample size of our series could bias these frequencies. KRAS mutations represented the most common mutated RAS gene in this series of UTUC, which contradicts the current literature since HRAS mutations are reported as more prevalent in the upper urinary tract cancer [98, 118, 119]. A possible explanation is the aggressiveness of the tumors that comprise this cohort. KRAS alterations are generally associated with tumors of higher grade and with a poorer prognosis, while the inverse occurs with HRAS alterations [86, 90]. Therefore, as previously mentioned, since this series is composed of tumors with more aggressive features (higher histological grade and T staging), a higher prevalence of KRAS mutations could be expected.

Another interesting finding was one of the identified KRAS alterations in this series. The p.V14I alteration is usually related to Noonan syndrome, which is an autosomal dominant genetic disorder characterized by craniofacial dysmorphism features, congenital heart defects, growth impairment and myeloproliferative disorders [120, 121]. Indeed, this germ-lime mutation is described as pathogenic in some tumors such as colorectal and lung cancers [120] but, to our knowledge, it still hasn't been reported in urothelial carcinoma, specifically in UTUC.

Several concomitant molecular alterations were identified in this series. Contrary to what the literature states, concomitant alterations were found between FGFR3 and RAS genes in 6 cases, which is unexpected since they are considered mutually exclusive events [74, 75, 91]. They appear to be early events in tumorigenesis [91], potentiating disease progression. These genes belong to the MAPK signaling pathway, FGFR3 as a tyrosine kinase receptor and RAS as a G-protein, and are responsible for activating a downstream cascade of tyrosine-kinases to promote cellular responses such as proliferation, differentiation and survival [74, 82, 86]. Therefore, this suggests that these mutations share a similar function and lead to a similar phenotype in UTUC, which seems redundant when both occur in the same tumor. A possible explanation is the presence of different clones

that could have acquired distinct mutations throughout time and gained new alternative means to progress and survive.

Previous studies reported that FGFR3 mutations tended to co-occur with TERTp mutations [94]. In our series, we observed overlapping of these mutations in 46 tumors which was statistically significant.

Additionally, 6 tumors were simultaneously mutated for both RAS and TERTp. A synergistic effect has been described between MAPK and TERTp mutations. Aberrant activation of the MAPK pathway can aid TERT in its role in senescence evasion by upregulating telomerase. ETS factors, one of ERK targets, bind to transcription factors binding motifs in the TERT promoter and stimulate TERT expression [85, 94, 99, 101].

Regarding the molecular results of 8 CIS samples, we observed a higher prevalence of FGFR3 mutations but no RAS or concomitant alterations were found. Discordant molecular profiles were found in two cases, of which in one case only the primary tumor presented two alterations (-124 C>T and p.G12D hotspots) and, in the other case, only the CIS presented -124 C>T alteration. These results are surprising since, from what we understand of bladder tumors, CIS lesions seem to follow a different genetic pathway, with an enrichment of TP53 mutations [49]. TP53 gene was not included in our genetic panel, but it could be interesting to evaluate later these mutations in CIS lesions.

For the descriptive analysis of 8 LN metastasis, the mutation frequency for FGFR3, TERTp and KRAS was 62.5%, 57.1% and 25.0%, respectively. Concomitant alterations were found in 3 tumors, of which one presented TERTp, FGFR3 and KRAS alterations. Moreover, 2 primary tumors and their respective LN metastases differed in molecular pattern and both LNM presented an extra alteration compared to the primary tumor. These discordant molecular profiles might be related to the heterogeneity of the tumor and the gain of extra mutations of the LNM could have influenced tumor dissemination and progression of the disease. Of note, LN metastases appeared to present more alterations than primary tumors. No further statistical analysis was performed for these lesions due to the very low number of samples.

Considering now the results obtained in the 114 patients we could also observe some correlations between molecular status and clinicopathological/follow-up characteristics. Specifically, for FGFR3 we found an association with the presence of these mutations and absence of lymphatic and venous invasion, supporting the current literature that reports FGFR3 as marker for better prognosis and survival [74, 95, 118]. No statistically significant associations were established between the overall RAS mutational status and clinicopathological characteristics, probably due to a low number of detected mutations.

NRAS alterations significantly correlated with younger patients age. The only patient that presented NRAS mutations was a male of 55 years old, which is a relatively young age considering all the other patients from this cohort. However, since only one NRAS mutation was found in this series, these results should be taken with caution.

Replicative immortality is one of the hallmarks of cancer and occurs in 80-90% of tumors [99, 103, 105]. Telomerase reactivation can occur through point mutations in the *TERT* promoter which increases TERT activity, gene expression and eventually cellular immortalization. These somatic mutations have been reported up to 80% of bladder tumours, across all stages and grades, and are associated with higher tumour progression and distant metastasis, leading to a poor prognosis and reduced survival rates in cancer [94, 99, 101, 104, 107]. Curiously, in the present series, TERTp alterations did not correlate with presence of distant metastasis nor other factors of poor prognosis. Although TERTp mutations are described as frequently altered in UTUC [100], associations with clinicopathological characteristics are still debatable in urothelial cancer and discordant reports exist on the literature; for example, Allory *et al*. [94] also described a lack of association between TERTp mutations and tumor progression in bladder cancer or development of metastases. But Wang *et al*. [104] found a correlation between these mutations and distant metastases in UTUC, suggesting a role in tumor dissemination. Therefore, a greater understanding of the impact of TERTp alterations in UTUC is of crucial importance.

To understand the role of molecular alterations in UTUC behavior and prognosis, we initially defined a multivariate model considering all significant variables related to the output, distant metastasis (staging M). However, regarding genetic alterations, we couldn't find any associations, probably due to the low number of distant metastases in our series. Therefore, when adjusting to a multivariate logistic model, we removed these variables and included lymphatic invasion, venous invasion and residual tumor (besides age and gender that were always added for proper adjustment), the variables significant in the univariate analysis. Venous invasion remained the only predictive factor for the development of distant metastasis. Of note, we observed that patients with tumors presenting venous invasion were 9.3 times more likely to develop distant metastases. This result is expected since circulating tumor cells mainly use the bloodstream to disseminate and form metastasis in organs distant from the primary tumor site [122].

The last part of our work was evaluating the expression pattern of CK5/6 and CK20, previously found altered in UTUC and supposed to be part of the recently proposed molecular subtypes of urothelial tumors [71, 72, 78]. Together with other markers, such as GATA3 and FOXA1, these biomarkers can add important prognostic clues.

Allied to the genetic alterations, expression patterns of molecular markers have been described as important surrogate and prognostic biomarkers in urothelial cancer. For example, in non-muscle-invasive high-grade UTUC, CK5/6-low/CK20-high was associated with a poor prognosis while the opposite cytokeratin pattern was correlated with an adverse outcome in muscle invasive carcinomas [113-115]. CK20 expression is normally found in urinary tissues but a strong expression is observed in the gastrointestinal tract and appendix. In contrast, CK5/6 expression is present in a wider range of tissues such as urinary bladder, prostate, skin and tonsil. Normal immunostaining for CK5/6 and CK20 is specific to the basal/intermediate and luminal layers of the transitional epithelium, respectively [110, 111, 114, 123].

We present here the preliminary results obtained in two of those biomarkers. We expected aberrant protein expression in our tumors and indeed we observed altered subcellular localization of both cytokeratins, with staining in all cell layers of the urothelium. Additionally, we identified immunostaining in the cytoplasm or in the cell membrane for all cases and no evidence of nuclear staining was found. Based on the score scheme we adopted (sum of intensity and proportion of positive-stained tumor cells), distinct expression patterns were observed ranging from a score of 0 to 6 for CK5/6 and 0 to 7 for CK20. As referred those results are still preliminary, and must be complemented with other biomarkers in order to be able to make assumptions and valid comparisons.

Statistical analysis was not performed comparing immunohistochemistry results with clinicopathological data nor genetic alterations as this is still an ongoing work which requires a more profound evaluation of the slides and a more complete database of the patient's reports. More tumors should be analyzed to increase the statistical value of our results and, ultimately, be able to differentiate luminal from basal-like tumors in further analyzes.

Conclusion and future perspectives

Upper urinary tract urothelial carcinoma is a rare neoplasm in developed countries, mainly affecting the male gender between 70 to 90 years of age. Due to its high aggressive biology, understanding the genetics of this disease remains of critical importance.

Our results suggest that genetic alterations could have a potential role in the patient's prognosis and survival. As observed with *FGFR*3 mutations, we found statistically significant associations between these alterations and absence of lymphatic and venous invasions which denotes their effect as good prognostic markers. We also assessed the molecular status of the *TERT*p but we found no associations with clinicopathological variables, contrary to previous reports. We did find concomitant alterations between *TERT*p/*FGFR*3 and *TERT*p/*RAS*, as expected. Although not performed in this study, it would be interesting to understand if concomitant mutations result in tumors with more aggressive features and worse prognosis, compared to single mutations. A larger sample size might contribute to a more powerful analysis and to a better understanding of how these molecular markers affect UTUC biology and clinical follow-up of each patient.

In the present series, we were not able to verify an impact of the studied genetic alterations on the development of distant metastases. However, we believe that the reduced number of patients harboring distant metastases present in our cases could have impacted these associations.

Additionally, further studies analyzing UTUC outcome and survival, as well as the recurrence data of these patients would give new insights of the effect between genetic alterations and disease aggressiveness. The lack of these follow-up data is an obvious limitation of our study that hinders the clinical relevance of our results. In the near future, we will try to surpass this by performing new multivariate analyses with survival and recurrence data.

Finally, our results regarding the expression patterns for CK5/6 and CK20 are still preliminary and constitute part of an ongoing project to be complemented with additional biomarkers.

References

1. Hall, J.E. and M.E. Hall, *The Urinary System: Functional Anatomy and Urine Formation by the Kidneys* in *Guyton and Hall Textbook of Medical Physiology*. 2021, Elsevier: Philadelphia, PA.
2. Hickling, D.R., T.T. Sun, and X.R. Wu, 2015, *Anatomy and Physiology of the Urinary Tract: Relation to Host Defense and Microbial Infection.* Microbiol Spectr. **3**(4).
3. Favorito, L.A., *Basic Embryology of Urogenital System*, in *Translational Research in Pediatric Urology: Basic and Clinical Aspects*, L.A. Favorito, Editor. 2021, Springer.
4. El-Galley, R.E. and T.E. Keane, 2000, *Embryology, anatomy, and surgical applications of the kidney and ureter.* Surgical Clinics of North America. **80**(1): p. 381-401.
5. Mahadevan, V., 2019, *Anatomy of the kidney and ureter.* Surgery (Oxford). **37**(7): p. 359-364.
6. Field, M., C. Pollock, and D. Harris, *Urinary tract structure and infection*, in *The Renal System: Systems of the Body Series*. 2010, Churchill Livingstone.
7. Smith, A.K., S.F. Matin, and T.W. Jarrett, *Urothelial Tumors of the Upper Urinary Tract and Ureter*, in *Campbell-Walsh urology*, L.R. Kavoussi, A.W. Partin, and C.A. Peters, Editors. 2016, Elsevier: Philadelphia, PA.
8. Kumar, V., A.K. Abbas, and J.C. Astar, *Kidney and Its Collecting System*, in *Robbins Basic Pathology*. 2018, Elsevier: Philadelphia, PA.
9. Wallace, M.A., 1998, *Anatomy and Physiology of the Kidney.* AORN Journal. **68**(5): p. 800, 803-16, 819-20; quiz 821-4.
10. Sampaio, F.J.B. and L.A. Favorito, *Basic Anatomy of Urinary Tract*, in *Translational Research in Pediatric Urology: Basic and Clinical Aspects*, L.A. Favorito, Editor. 2021, Springer.
11. Lierse, W., et al., *Special Part: I - The Kidneys (Renes)*, in *Applied Anatomy of the Pelvis*, J. Lang and W. Wachsmuth, Editors. 1987, Springer: Berlin.
12. Elkoushy, M.A. and S. Andonian, *Surgical, Radiologic, and Endoscopic Anatomy of the Kidney and Ureter*, in *Campbell-Walsh urology*, L.R. Kavoussi, A.W. Partin, and C.A. Peters, Editors. 2016, Elsevier: Philadelphia, PA.
13. Standring, S., et al., *Kidney and ureter*, in *Gray's Anatomy*. 2016, Elsevier.
14. Lierse, W., et al., *Special Part: II - Renal Pelvis*, in *Applied anatomy of the Pelvis*, J. Lang and W. Wachsmuth, Editors. 1987, Springer: Berlin.
15. Schmidt-Nielsen, B., 1987, *The renal pelvis.* Kidney International. **31**(2): p. 621-8.
16. Lierse, W., et al., *Special Part: III - Ureter*, in *Applied anatomy of the Pelvis*, J. Lang and W. Wachsmuth, Editors. 1987, Springer: Berlin.

17. Woldemeskel, M., W. Drommer, and M. Wendt, 1998, *Histology and ultrastructure of the urothelium lining the ureter and the renal pelvis in sows.* Anatomia, Histologia, Embryologia. **27**(1): p. 51-5.
18. Van Der Poel, H.G., et al., 2005, *Upper urinary tract cancer: location is correlated with prognosis.* European Urology. **48**(3): p. 438-44.
19. *Upper Tract Urothelial Carcinoma*, ed. S.F. Shariat and E. Xylinas. 2015, New York: Springer.
20. Seçil, M. and G.T. Maclennan, *Neoplasms of the Renal Pelvis and Ureter*, in *Genitourinary Radiology: Kidney, Bladder and Urethra*, V.S. Dogra and G.T. MacLennan, Editors. 2013, Springer: London.
21. Rouprêt, M., et al., 2021, *European Association of Urology Guidelines on Upper Urinary Tract Urothelial Carcinoma: 2020 Update.* European Urology. **79**(1): p. 62-79.
22. Siegel, R.L., et al., 2021, *Cancer Statistics, 2021.* CA: A Cancer Journal for Clinicians. **71**(1): p. 7-33.
23. Petros, F.G., 2020, *Epidemiology, clinical presentation, and evaluation of upper-tract urothelial carcinoma.* Translational Andrology and Urology. **9**(4): p. 1794-1798.
24. Gupta, R., G.P. Paner, and M.B. Amin, 2008, *Neoplasms of the upper urinary tract: a review with focus on urothelial carcinoma of the pelvicalyceal system and aspects related to its diagnosis and reporting.* Advances in Anatomic Pathology. **15**(3): p. 127-39.
25. Genega, E.M. and C.R. Porter, 2002, *Urothelial neoplasms of the kidney and ureter. An epidemiologic, pathologic, and clinical review.* American Journal of Clinical Pathology. **117** Suppl:S36-48.
26. Raman, J.D., et al., 2011, *Incidence and survival of patients with carcinoma of the ureter and renal pelvis in the USA, 1973-2005.* BJU International. **107**(7): p. 1059-64.
27. Wu, Y., et al., 2014, *The impact of tumor location and multifocality on prognosis for patients with upper tract urothelial carcinoma: a meta-analysis.* Scientific Reports. **4**: p. 6361.
28. Fang, D., et al., 2018, *Comparison of clinicopathologic characteristics, epigenetic biomarkers and prognosis between renal pelvic and ureteral tumors in upper tract urothelial carcinoma.* BMC Urology. **18**(1): p. 22.
29. Ouzzane, A., et al., 2011, *Ureteral and multifocal tumours have worse prognosis than renal pelvic tumours in urothelial carcinoma of the upper urinary tract treated by nephroureterectomy.* European Urology. **60**(6): p. 1258-65.

30. Shariat, S.F., et al., 2011, *Gender differences in radical nephroureterectomy for upper tract urothelial carcinoma.* World Journal of Urology. **29**(4): p. 481-6.
31. Soria, F., et al., 2017, *Epidemiology, diagnosis, preoperative evaluation and prognostic assessment of upper-tract urothelial carcinoma (UTUC).* World Journal of Urology. **35**(3): p. 379-387.
32. Choudhury, M.S., *Epidemiology and Presentation*, in *Urothelial Malignancies of the Upper Urinary Tract*, M. Eshghi, Editor. 2018, Springer.
33. American Cancer Society, A.C., 2021, *Cancer Facts & Figures 2021.* Atlanta: American Cancer Society.
34. Roberts, J.L., et al., 2019, *Diagnosis, management, and follow-up of upper tract urothelial carcinoma: an interdisciplinary collaboration between urology and radiology.* Abdominal Radiology (NY). **44**(12): p. 3893-3905.
35. Margulis, V., et al., 2009, *Outcomes of radical nephroureterectomy: a series from the Upper Tract Urothelial Carcinoma Collaboration.* Cancer. **115**(6): p. 1224-33.
36. Howlader, N. *SEER Cancer Statistics Review*. 1975-2018 [cited 2021 May]; Available from: https://seer.cancer.gov/csr/1975_2016/.
37. Munoz, J.J. and L.M. Ellison, 2000, *Upper tract urothelial neoplasms: incidence and survival during the last 2 decades.* Journal of Urology. **164**(5): p. 1523-5.
38. RORENO, 2016, *Registo Oncológico Nacional 2010.* Instituto Português de Oncologia do Porto Francisco Gentil - EPE.
39. Colin, P., et al., 2009, *Environmental factors involved in carcinogenesis of urothelial cell carcinomas of the upper urinary tract.* BJU International. **104**(10): p. 1436-40.
40. Mclaughlin, J.K., 1992, *Cigarette smoking and cancers of the renal pelvis and ureter.* Cancer Research. **52**(2): p. 254-7.
41. Shinka, T., 1995, *Factors affecting the occurrence of urothelial tumors in dye workers exposed to aromatic amines.* International Journal of Urology. **2**(4): p. 243-8.
42. Skeldon, S.C., et al., 2013, *Patients with Lynch syndrome mismatch repair gene mutations are at higher risk for not only upper tract urothelial cancer but also bladder cancer.* European Urology. **63**(2): p. 379-85.
43. Van Der Post, R.S., et al., 2010, *Risk of urothelial bladder cancer in Lynch syndrome is increased, in particular among MSH2 mutation carriers.* Journal of Medical Genetics. **47**(7): p. 464-70.
44. Audenet, F., et al., 2012, *A proportion of hereditary upper urinary tract urothelial carcinomas are misclassified as sporadic according to a multi-institutional database analysis: proposal of patient-specific risk identification tool.* BJU International. **110**(11 Pt B): p. E583-9.

45. Lughezzani, G., et al., 2012, *Prognostic factors in upper urinary tract urothelial carcinomas: a comprehensive review of the current literature.* European Urology. **62**(1): p. 100-14.
46. Meldrum, K.K., *Pathophysiology of Urinary Tract Obstruction*, in *Campbell-Walsh urology*, L.R. Kavoussi, A.W. Partin, and C.A. Peters, Editors. 2016, Elsevier: Philadelphia, PA.
47. Steenbergen, S.L. and G. Israel, *Imaging of Upper Tract Transitional Cell Carcinoma*, in *Upper Urinary Tract Urothelial Carcinoma*, M. Grasso III and D.H. Bagley, Editors. 2015, Springer.
48. Akhavein, A. and M. Monga, *Semirigid and Flexible Ureteroscopy*, in *Urothelial Malignancies of the Upper Urinary Tract*, M. Eshghi, Editor. 2018, Springer.
49. Batista, R., et al., 2020, *Biomarkers for Bladder Cancer Diagnosis and Surveillance: A Comprehensive Review.* Diagnostics (Basel). **10**(1): p. 39.
50. Mehrazin, R. and C.A. Olsson, *Open Nephroureterectomy*, in *Urothelial Malignancies of the Upper Urinary Tract*, M. Eshghi, Editor. 2018, Springer.
51. Chou, Y.H., et al., 2013, *The association between gender and outcome of patients with upper tract urothelial cancer.* Kaohsiung J Med Sci. **29**(1): p. 37-42.
52. Alifrangis, C., et al., 2019, *Molecular and histopathology directed therapy for advanced bladder cancer.* Nat Rev Urol. **16**(8): p. 465-483.
53. Conlin, M.J. and B.D. Duty, *Surveillance After Treatment for Upper Tract Transitional Cell Carcinoma*, in *Upper Urinary Tract Urothelial Carcinoma*, M. Grasso III and D.H. Bagley, Editors. 2015, Springer.
54. Van Osch, F.H., et al., 2016, *Significant Role of Lifetime Cigarette Smoking in Worsening Bladder Cancer and Upper Tract Urothelial Carcinoma Prognosis: A Meta-Analysis.* Journal of Urology. **195**(4 Pt 1): p. 872-9.
55. Mbeutcha, A., et al., *Prognostic Factors and Predictive Tools in Upper Tract Urothelial Carcinoma*, in *Urothelial Malignancies of the Upper Urinary Tract*, M. Eshghi, Editor. 2018, Springer.
56. Ehdaie, B., et al., 2011, *Obesity adversely impacts disease specific outcomes in patients with upper tract urothelial carcinoma.* Journal of Urology. **186**(1): p. 66-72.
57. Milojevic, B., et al., 2013, *Prognostic significance of non-muscle-invasive bladder tumor history in patients with upper urinary tract urothelial carcinoma.* Urologic Oncology. **31**(8): p. 1615-20.
58. Favaretto, R.L., et al., 2010, *The effect of tumor location on prognosis in patients treated with radical nephroureterectomy at Memorial Sloan-Kettering Cancer Center.* European Urology. **58**(4): p. 574-80.

59. Isbarn, H., et al., 2009, *Location of the primary tumor is not an independent predictor of cancer specific mortality in patients with upper urinary tract urothelial carcinoma.* Journal of Urology. **182**(5): p. 2177-81.
60. Park, S., et al., 2004, *The impact of tumor location on prognosis of transitional cell carcinoma of the upper urinary tract.* Journal of Urology. **171**(2 Pt 1): p. 621-5.
61. Williams, A.K., et al., 2013, *Multifocality rather than tumor location is a prognostic factor in upper tract urothelial carcinoma.* Urologic Oncology. **31**(7): p. 1161-5.
62. Zhang, X.K., et al., 2015, *Tumor necrosis predicts poor clinical outcomes in patients with node-negative upper urinary tract urothelial carcinoma.* Japanese Journal of Clinical Oncology. **45**(11): p. 1069-75.
63. Langner, C., et al., 2006, *pT classification, grade, and vascular invasion as prognostic indicators in urothelial carcinoma of the upper urinary tract.* Modern Pathology. **19**(2): p. 272-9.
64. Winer, A.G., et al., 2017, *Prognostic value of lymph node yield during nephroureterectomy for upper tract urothelial carcinoma.* Urologic Oncology. **35**(4): p. 151 e9-151 e15.
65. Humphrey, P.A., et al., 2016, *The 2016 WHO Classification of Tumours of the Urinary System and Male Genital Organs-Part B: Prostate and Bladder Tumours.* European Urology. **70**(1): p. 106-119.
66. Hajiyeva, S. and M. Zhong, *Pathology of Urothelial Malignancies of the Upper Urinary Tract*, in *Urothelial Malignancies of the Upper Urinary Tract*, M. Eshghi, Editor. 2018, Springer.
67. Mckenney, J.K., *Classification and Histologic Grading of Urothelial Neoplasms by the WHO 2004 (ISUP 1998) Criteria*, in *Genitourinary Pathology*, C. Magi-Galluzzi and C.G. Przybycin, Editors. 2015, Springer: New York.
68. Kumar, V., A.K. Abbas, and J.C. Astar, *Male Genital System and Lower Urinary Tract*, in *Robbins Basic Pathology*. 2018, Elsevier: Philadelphia, PA.
69. Montironi, R., et al., 2009, *2004 World Health Organization Classification of the Noninvasive Urothelial Neoplasms: Inherent Problems and Clinical Reflections.* European Urology Supplements. **8**(5): p. 453-457.
70. Soukup, V., et al., 2017, *Prognostic Performance and Reproducibility of the 1973 and 2004/2016 World Health Organization Grading Classification Systems in Non-muscle-invasive Bladder Cancer: A European Association of Urology Non-muscle Invasive Bladder Cancer Guidelines Panel Systematic Review.* European Urology. **72**(5): p. 801-813.
71. Guo, C.C., et al., 2020, *Assessment of Luminal and Basal Phenotypes in Bladder Cancer.* Scientific Reports. **10**(1): p. 9743.

72. Mcconkey, D.J. and W. Choi, 2018, *Molecular Subtypes of Bladder Cancer.* Current Oncology Reports. **20**(10): p. 77.
73. Guo, C.C. and B. Czerniak, 2019, *Bladder Cancer in the Genomic Era.* Archives of Pathology and Laboratory Medicine. **143**(6): p. 695-704.
74. Di Martino, E., et al., 2016, *A place for precision medicine in bladder cancer: targeting the FGFRs.* Future Oncology. **12**(19): p. 2243-63.
75. Jebar, A.H., et al., 2005, *FGFR3 and Ras gene mutations are mutually exclusive genetic events in urothelial cell carcinoma.* Oncogene. **24**(33): p. 5218-25.
76. Kompier, L.C., et al., 2010, *FGFR3, HRAS, KRAS, NRAS and PIK3CA Mutations in Bladder Cancer and Their Potential as Biomarkers for Surveillance and Therapy.* PloS One. **5**(11): p. e13821.
77. Dadhania, V., et al., 2016, *Meta-Analysis of the Luminal and Basal Subtypes of Bladder Cancer and the Identification of Signature Immunohistochemical Markers for Clinical Use.* EBioMedicine. **12**: p. 105-117.
78. Choi, W., et al., 2014, *Identification of distinct basal and luminal subtypes of muscle-invasive bladder cancer with different sensitivities to frontline chemotherapy.* Cancer Cell. **25**(2): p. 152-65.
79. Robertson, A.G., et al., 2017, *Comprehensive Molecular Characterization of Muscle-Invasive Bladder Cancer.* Cell. **171**(3): p. 540-556 e25.
80. Robinson, B.D., et al., 2019, *Upper tract urothelial carcinoma has a luminal-papillary T-cell depleted contexture and activated FGFR3 signaling.* Nat Commun. **10**(1): p. 2977.
81. Moss, T.J., et al., 2017, *Comprehensive Genomic Characterization of Upper Tract Urothelial Carcinoma.* European Urology. **72**(4): p. 641-649.
82. Santarpia, L., S.M. Lippman, and A.K. El-Naggar, 2012, *Targeting the MAPK-RAS-RAF signaling pathway in cancer therapy.* Expert Opinion on Therapeutic Targets. **16**(1): p. 103-19.
83. Korzeniecki, C. and R. Priefer, 2021, *Targeting KRAS mutant cancers by preventing signaling transduction in the MAPK pathway.* European Journal of Medicinal Chemistry. **211**: p. 113006.
84. Dhillon, A.S., et al., 2007, *MAP kinase signalling pathways in cancer.* Oncogene. **26**(22): p. 3279-90.
85. Neuzillet, C., et al., 2014, *MEK in cancer and cancer therapy.* Pharmacol Ther. **141**(2): p. 160-71.

86. Smal, M.P., et al., 2016, *The opposite association of HRAS and KRAS mutations with clinical variables of bladder cancer.* Russian Journal of Genetics: Applied Research. **6**(5): p. 613-621.
87. Zhang, W. and H. Liu, 2002, *MAPK signal pathways in the regulation of cell proliferation in mammalian cells.* Cell Research. **12**(1): p. 9-18.
88. Tidyman, W.E. and K.A. Rauen, 2016, *Pathogenetics of the RASopathies.* Human Molecular Genetics. **25**(R2): p. R123-R132.
89. Fang, J.Y. and B.C. Richardson, 2005, *The MAPK signalling pathways and colorectal cancer.* The Lancet Oncology. **6**(5): p. 322-327.
90. Tripathi, K., et al., 2020, *Mutational analysis of Ras hotspots in patients with urothelial carcinoma of the bladder.* World Journal of Clinical Oncology. **11**(8): p. 614-628.
91. Knowles, M.A., 2007, *Role of FGFR3 in urothelial cell carcinoma: biomarker and potential therapeutic target.* World Journal of Urology. **25**(6): p. 581-93.
92. Gómez-Román, J.J., et al., 2005, *Fibroblast growth factor receptor 3 is overexpressed in urinary tract carcinomas and modulates the neoplastic cell growth.* Clin Cancer Res. **11**(2 Pt 1): p. 459-65.
93. Touat, M., et al., 2015, *Targeting FGFR Signaling in Cancer.* Clin Cancer Res. **21**(12): p. 2684-94.
94. Allory, Y., et al., 2014, *Telomerase reverse transcriptase promoter mutations in bladder cancer: high frequency across stages, detection in urine, and lack of association with outcome.* European Urology. **65**(2): p. 360-6.
95. Van Oers, J.M., et al., 2009, *FGFR3 mutations indicate better survival in invasive upper urinary tract and bladder tumours.* European Urology. **55**(3): p. 650-7.
96. Prior, I.A., P.D. Lewis, and C. Mattos, 2012, *A comprehensive survey of Ras mutations in cancer.* Cancer Research. **72**(10): p. 2457-67.
97. Audenet, F., et al., 2019, *Clonal Relatedness and Mutational Differences between Upper Tract and Bladder Urothelial Carcinoma.* Clin Cancer Res. **25**(3): p. 967-976.
98. Necchi, A., et al., 2020, *Comprehensive Genomic Profiling of Upper-tract and Bladder Urothelial Carcinoma.* Eur Urol Focus.
99. Wang, K., 2014, *TERT promoter mutations in renal cell carcinomas and upper tract urothelial carcinomas.* Oncotarget. **5**(7): p. 1829-1836.
100. Killela, P.J., et al., 2013, *TERT promoter mutations occur frequently in gliomas and a subset of tumors derived from cells with low rates of self-renewal.* Proceedings of the National Academy of Sciences. **110**(15): p. 6021-6026.

101. Yuan, X., M. Dai, and D. Xu, 2020, *TERT promoter mutations and GABP transcription factors in carcinogenesis: More foes than friends.* Cancer Letters. **493**: p. 1-9.
102. Kim, N.W., 1994, *Specific association of human telomerase activity with immortal cells and cancer.* Science. **266**(5193): p. 2011-5.
103. Borah, S., et al., 2015, *TERTpromoter mutations and telomerase reactivation in urothelial cancer.* Science. **347**(6225): p. 1006-1010.
104. Wang, K., 2014, *TERT promoter mutations are associated with distant metastases in upper tract urothelial carcinomas and serve as urinary biomarkers detected by a sensitive castPCR.* Oncotarget. **5**(23): p. 12428-39.
105. Hanahan, D. and R.A. Weinberg, 2011, *Hallmarks of cancer: the next generation.* Cell. **144**(5): p. 646-74.
106. Vinagre, J., et al., 2013, *Frequency of TERT promoter mutations in human cancers.* Nat Commun. **4**: p. 2185.
107. Kinde, I., et al., 2013, *TERT promoter mutations occur early in urothelial neoplasia and are biomarkers of early disease and disease recurrence in urine.* Cancer Research. **73**(24): p. 7162-7.
108. Heidenreich, B. and R. Kumar, 2017, *TERT promoter mutations in telomere biology.* Mutat Res Rev Mutat Res. **771**: p. 15-31.
109. Sanguedolce, F., et al., 2019, *Diagnostic and prognostic roles of CK20 in the pathology of urothelial lesions. A systematic review.* Pathology, Research and Practice. **215**(6): p. 152413.
110. Breyer, J., et al., 2017, *In stage pT1 non-muscle-invasive bladder cancer (NMIBC), high KRT20 and low KRT5 mRNA expression identify the luminal subtype and predict recurrence and survival.* Virchows Archiv. **470**(3): p. 267-274.
111. Gil Da Costa, R.M., et al., 2015, *Altered expression of CKs 14/20 is an early event in a rat model of multistep bladder carcinogenesis.* International Journal of Experimental Pathology. **96**(5): p. 319-25.
112. Moll, R., 1992, *Cytokeratin 20 in human carcinomas. A new histodiagnostic marker detected by monoclonal antibodies.* The American Journal of Pathology. **140**(2): p. 427-47.
113. Akhtar, M., et al., 2020, *CK20 and CK5/6 Immunohistochemical Staining of Urothelial Neoplasms: A Perspective.* Adv Urol. **2020**: p. 4920236.
114. Jangir, H., et al., 2019, *Prognostic stratification of muscle invasive urothelial carcinomas using limited immunohistochemical panel of Gata3 and cytokeratins 5/6, 14 and 20.* Annals of Diagnostic Pathology. **43**: p. 151397.

115. Jung, M., B. Kim, and K.C. Moon, 2019, *Immunohistochemistry of cytokeratin (CK) 5/6, CD44 and CK20 as prognostic biomarkers of non-muscle-invasive papillary upper tract urothelial carcinoma.* Histopathology. **74**(3): p. 483-493.
116. Yin, H. and A.S.Y. Leong, 2004, *Histologic Grading of Noninvasive Papillary Urothelial Tumors.* American Journal of Clinical Pathology. **121**(5): p. 679-687.
117. Harnden, P., N. Mahmood, and J. Southgate, 1999, *Expression of cytokeratin 20 redefines urothelial papillomas of the bladder.* The Lancet. **353**(9157): p. 974-977.
118. Li, Q., et al., 2016, *Prognostic Genetic Signatures in Upper Tract Urothelial Carcinoma.* Curr Urol Rep. **17**(2): p. 12.
119. Sfakianos, J.P., et al., 2015, *Genomic Characterization of Upper Tract Urothelial Carcinoma.* European Urology. **68**(6): p. 970-7.
120. Hernandez-Porras, I., et al., 2014, *K-RasV14I recapitulates Noonan syndrome in mice.* Proceedings of the National Academy of Sciences of the United States of America. **111**(46): p. 16395-400.
121. Bera, A.K., et al., 2019, *Structural basis of the atypical activation mechanism of KRAS(V14I).* Journal of Biological Chemistry. **294**(38): p. 13964-13972.
122. San Juan, B.P., et al., 2019, *The Complexities of Metastasis.* Cancers. **11**(10).
123. Akhtar, M., et al., 2020, *CK20 and CK5/6 Immunohistochemical Staining of Urothelial Neoplasms: A Perspective.* Advances in Urology. **2020**: p. 4920236.

Supplementary data

Supplementary Table I. Associations between clinicopathological features and clinical follow-up data of primary tumors.

Parameters	Parameters												
	Age	**Gender**	**Tumor location**	**Tumor side**	**Epithelial associated lesions**	**Lymphatic invasion**	**Venous invasion**	**Tumor grade**	**Staging T**	**Staging N**	**Staging M**	**Procedure**	**Residual tumor**
	p-value	p-value	p-value	p-value	p-value	p-value	p-value	p-value	p-value	p-value	p-value	p-value	p-value
Age		0.085	0.556	0.709	0.391	0.062	**0.037**	0.480	0.347	0.997	0.445	0.093	**0.004**
Gender			0.087	0.500	0.439	0.683	1.000	0.363	0.949	0.964	0.528	0.876	0.893
Tumor location				0.995	0.760	0.779	0.142	0.836	0.550	0.977	0.989	**0.004**	0.265
Tumor side					0.978	0.478	0.640	0.845	0.550	0.551	0.676	0.809	0.935
Epithelial associated lesions						**0.031**	**0.049**	0.197	0.999	0.119	0.682	0.973	0.848
Lymphatic invasion							**<0.001**	0.073	**<0.001**	0.111	**0.006**	0.935	0.516
Venous invasion								0.094	**<0.001**	0.224	**<0.001**	0.918	**0.004**
Tumor grade									**<0.001**	0.237	0.416	**<0.001**	0.752
Staging T										0.392	**0.002**	0.341	0.283
Staging N											0.826	**0.001**	0.264
Staging M												0.545	**0.037**
Procedure													0.084
Residual tumor													

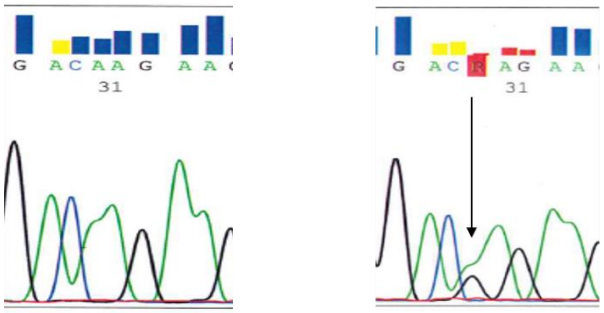

Supplementary Figure I. Representative sanger sequencing chromatogram of WT and mutated NRAS hotspots.

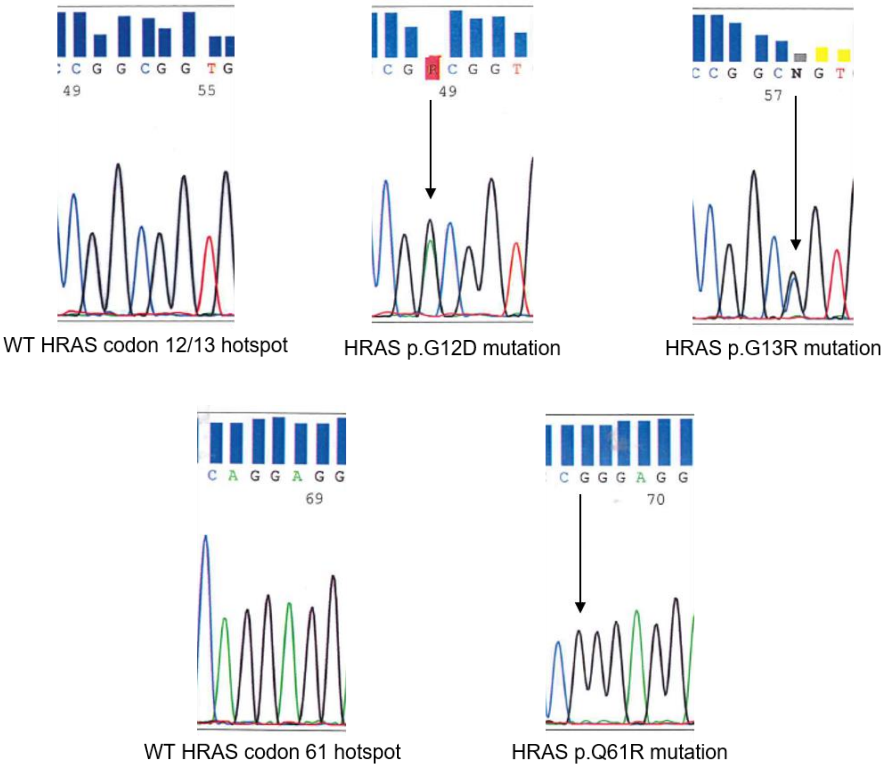

Supplementary Figure II. Representative sanger sequencing chromatogram of WT and mutated HRAS hotspots.

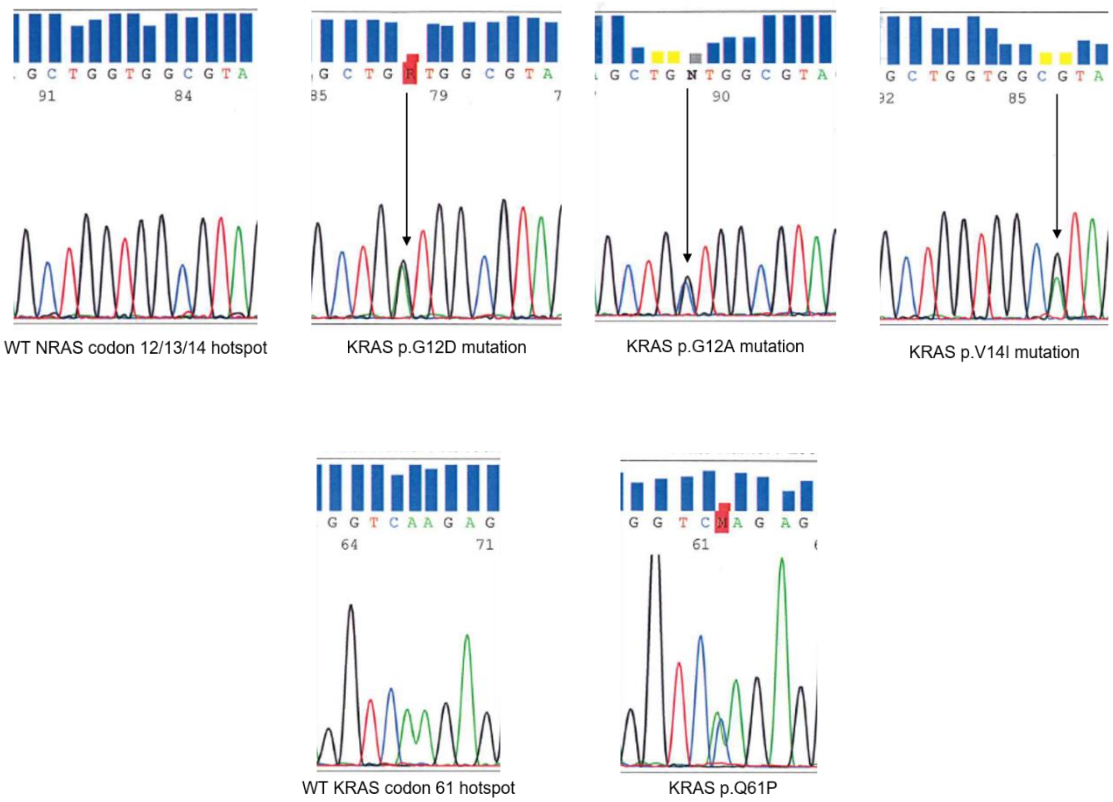

Supplementary Figure III. Representative sanger sequencing chromatogram of WT and mutated KRAS hotspots.

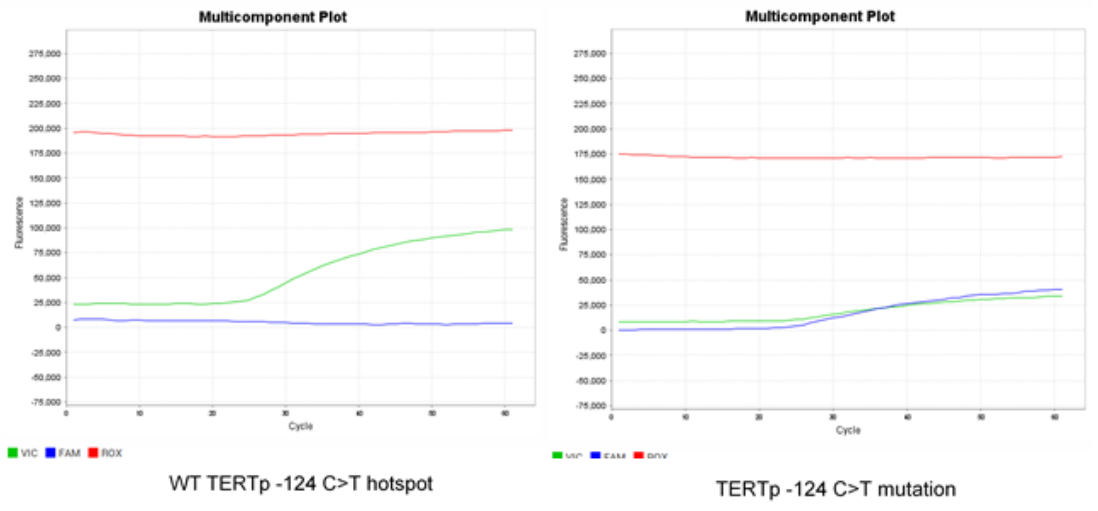

Supplementary Figure IV. Representative chromatogram of WT and mutated TERTp hotspots.

(Continued)

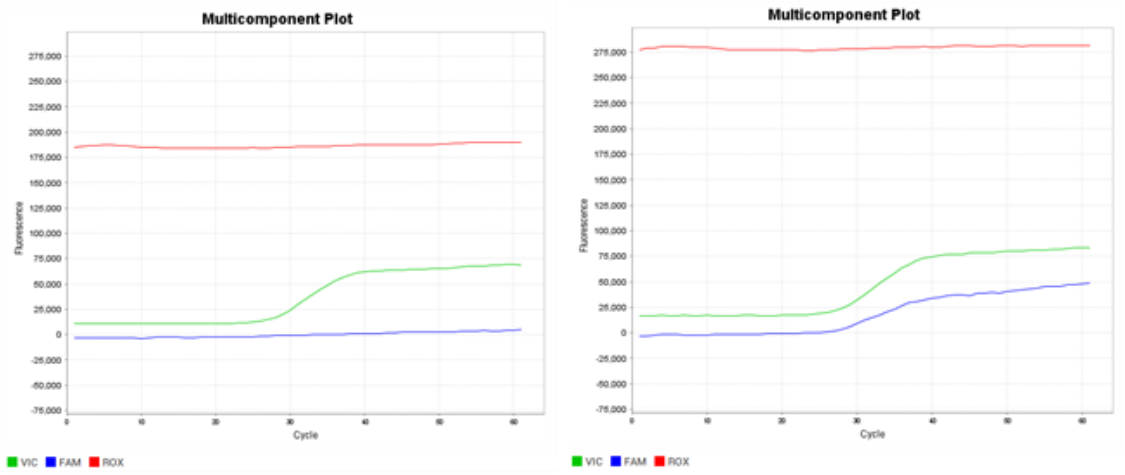

Supplementary Figure IV. Continued.

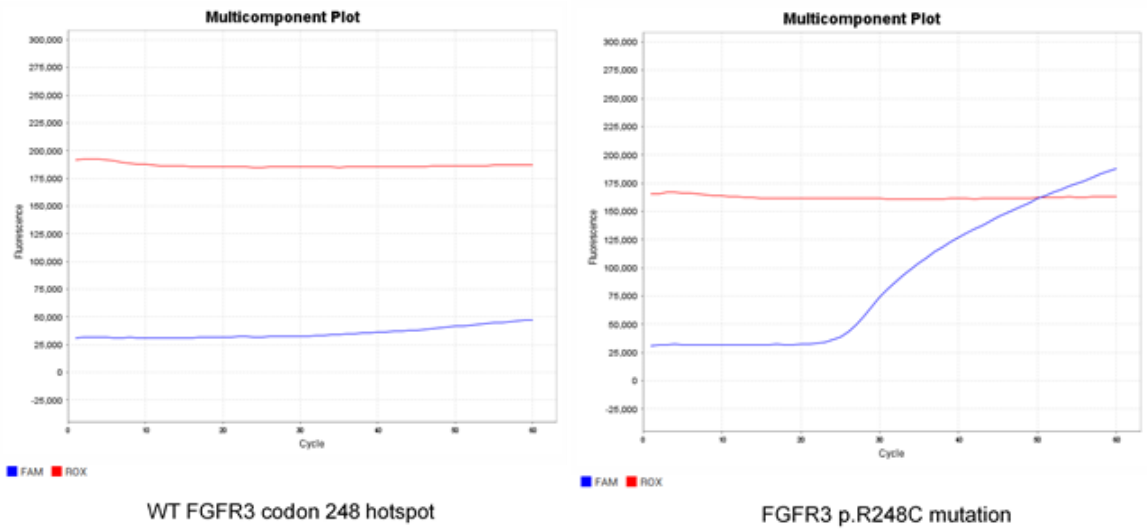

Supplementary Figure V. Representative chromatogram of WT and mutated FGFR3 hotspots.

(Continued)

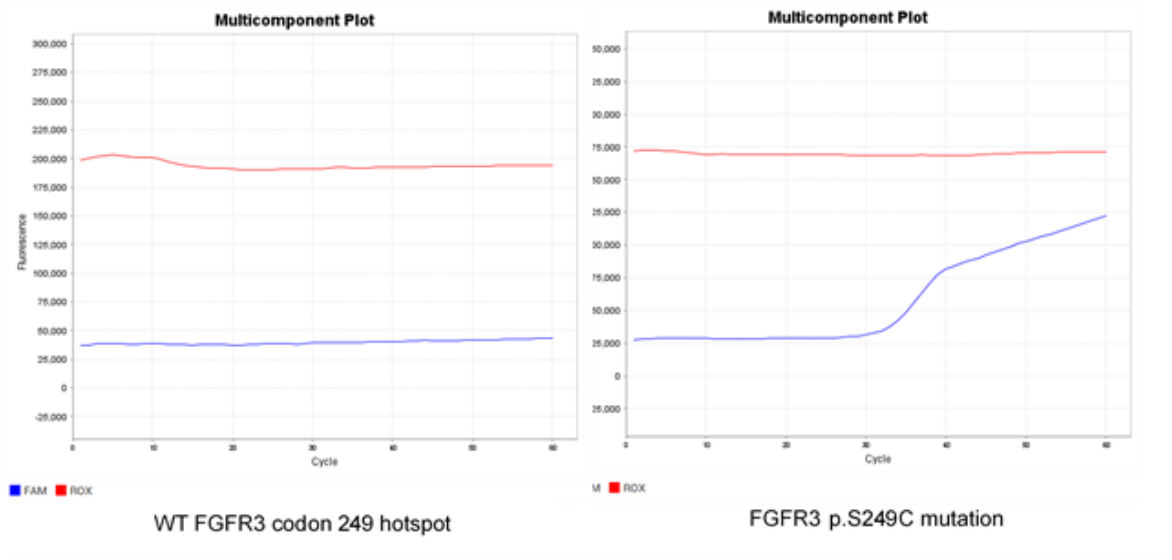

Supplementary Figure V. Continued.

Supplementary Table II. TERTp and FGFR3 status

		FGFR3 status	
		WT	**Mutated**
TERTp status	**WT**	33	26
	Mutated	25	46

Supplementary Table III. TERTp and RAS status

		RAS status	
		WT	**Mutated**
TERTp status	**WT**	54	6
	Mutated	65	6

Supplementary Table IV. FGFR3 and RAS status

		RAS status	
		WT	**Mutated**
FGFR3 status	**WT**	55	6
	Mutated	70	6

Supplementary Table V. Genetic alterations in carcinomas in situ.

Genes	n	WT	Mutated	Mutation type
***TERT*p**	4*	3 (75.0%)	1 (25.0%)	1 (-124 C>T)
FGFR3	5*	3 (60.0%)	2 (40.0%)	1 (p.R248C) 1 (p.S249C)
NRAS	8	8 (100%)	0 (0%)	-
HRAS	8	8 (100%)	0 (0%)	-
KRAS	8	8 (100%)	0 (0%)	-

*Total number of cases lower than 8 due to technical issues

Supplementary Table VI. Univariate analysis for TERTp mutations status and clinicopathological characteristics of primary tumors

Parameters	***TERT*p**		p-value
	WT	Mutated	
Clinicopathological features			
Age, mean ± SD (n=110)	76.70 ± 12.26	78.70 ± 9.74	0.304
Gender (n=110)			
Female	15 (31.9%)	17 (27.0%)	0.573
Male	32 (68.1%)	46 (73.0%)	
Tumor location (n=110)			
Renal pelvis	25 (53.2%)	41 (65.1%)	
Ureter	16 (34.0%)	15 (23.8%)	0.428
Multiple	6 (12.8%)	7 (11.1%)	
Tumor side (n=110)			
Right	23 (48.9%)	36 (57.1%)	0.393
Left	24 (51.1%)	27 (42.9%)	
Epithelial associated lesions (n=108)*			
Absent	37 (78.7%)	50 (82.0%)	0.673
Present	10 (21.3%)	11 (18.0%)	
Lymphatic invasion (n=106)*			
Absent	32 (71.1%)	44 (72.1%)	0.908
Present	13 (28.9%)	17 (27.9%)	

* Total number of cases lower than 110 due to missing clinical information

(Continued)

Supplementary Table VI – Continued.

Parameters	*TERT*p		p-value
	WT	Mutated	
Clinicopathological features			
Venous invasion (n=106)*			
Absent	32 (71.1%)	47 (77.0%)	0.488
Present	13 (28.9%)	14 (23.0%)	
Clinical-follow up			
Tumor grade (n=108)*			
Low	4 (8.9%)	3 (4.8%)	0.390
High	41 (91.1%)	60 (95.2%)	
Staging T (n=109)*			
Ta / Tis	3 (6.5%)	4 (6.3%)	
T1	12 (26.1%)	14 (22.2%)	
T2	8 (17.4%)	11 (17.5%)	0.951
T3	21 (45.7%)	29 (46.0%)	
T4	2 (4.3%)	5 (7.9%)	
Staging N (n=105)*			
N0/Nx	43 (93.5%)	55 (93.2%)	0.830
N1	2 (4.3%)	3 (5.1%)	
N2	1 (2.2%)	1 (1.7%)	
Staging M (n=93)*			
M0/Mx	36 (87.8%)	46 (88.5%)	0.922
M1	5 (12.2%)	6 (11.5%)	
Treatment procedure (n=110)			
Nephroureterectomy	43 (91.5%)	58 (92.1%)	0.196
Partial ureterectomy	2 (4.3%)	5 (7.9%)	
Nephroscopy with resection	2 (4.3%)	0 (0%)	
Residual tumor (n=106)*			
R0	38 (82.6%)	55 (91.7%)	0.299
R1	5 (10.9%)	4 (6.7%)	
R2	3 (6.5%)	1 (1.7%)	

* Total number of cases lower than 110 due to missing clinical information

Supplementary Table VII. Univariate analysis for FGFR3 mutations status and clinicopathological characteristics of primary tumors

Parameters	*FGFR3*		p-value
	WT	Mutated	
Clinicopathological features			
Age, mean ± SD (n=113)	77.88 ± 10.53	77.48 ± 11.39	0.848
Gender (n=113)			
Female	14 (27.5%)	19 (30.6%)	0.710
Male	37 (72.5%)	43 (69.4%)	
Tumor location (n=113)			
Renal pelvis	31 (60.8%)	38 (61.3%)	0.567
Ureter	12 (23.5%)	18 (29.0%)	
Multiple	8 (15.7%)	6 (9.7%)	
Tumor side (n=113)			
Right	26 (51.0%)	33 (53.2%)	0.812
Left	25 (49.0%)	29 (46.8%)	
Epithelial associated lesions (n=111)*			
Absent	38 (74.5%)	52 (86.7%)	0.103
Present	13 (25.5%)	8 (13.3%)	
Lymphatic invasion (n=109)*			
Absent	27 (55.1%)	49 (81.7%)	**0.003**
Present	22 (44.9%)	11 (18.3%)	
Venous invasion (n=109)*			
Absent	28 (57.1%)	51 (85.9%)	**0.001**
Present	21 (42.9%)	9 (15.0%)	
Clinical-follow up			
Tumor grade (n=111)*			
Low	2 (4.1%)	5 (8.1%)	0.391
High	47 (95.9%)	57 (91.9%)	

* Total number of cases lower than 113 due to missing clinical information

(Continued)

Supplementary Table VII – Continued.

Parameters	*FGFR3*		p-value
	WT	Mutated	
Clinical-follow up			
Staging T (n=112)*			
Ta / Tis	2 (4.0%)	5 (8.1%)	
T1	9 (18.0%)	17 (27.4%)	
T2	8 (16.0%)	11 (17.7%)	0.541
T3	26 (52.0%)	25 (40.3%)	
T4	5 (10%)	4 (6.5%)	
Staging N (n=108)*			
N0/Nx	47 (94%)	53 (91.4%)	
N1	2 (4%)	4 (6.9%)	0.811
N2	1 (2%)	1 (1.7%)	
Staging M (n=97)*			
M0/Mx	39 (86.7%)	45 (86.5%)	0.985
M1	6 (13.3%)	7 (13.5%)	
Treatment procedure (n=113)			
Nephroureterectomy	46 (90.2%)	59 (95.2%)	
Partial ureterectomy	3 (5.9%)	3 (4.8%)	0.278
Nephroscopy with resection	2 (3.9%)	0 (0%)	
Residual tumor (n=109)*			
R0	42 (84.0%)	53 (89.8%)	
R1	5 (10.0%)	5 (8.5%)	0.463
R2	3 (6.0%)	1 (1.7%)	

* Total number of cases lower than 113 due to missing clinical information

Supplementary Table VIII. Univariate analysis for RAS mutations status and clinicopathological characteristics of primary tumors

Parameters	*RAS*		p-value
	WT	Mutated	
Clinicopathological features			
Age, mean ± SD (n=114)	77.56 ± 10.58	79.18 ± 14.34	0.643
Gender (n=114)			
Female	31 (30.1%)	2 (18.2%)	0.408
Male	72 (69.9%)	9 (81.8%)	
Tumor location (n=114)			
Renal pelvis	61 (59.2%)	8 (72.7%)	
Ureter	29 (28.2%)	2 (18.2%)	0.682
Multiple	13 (12.6%)	1 (9.1%)	
Tumor side (n=114)			
Right	56 (54.4%)	4 (36.4%)	0.256
Left	47 (45.6%)	7 (63.6%)	
Epithelial associated lesions (n=112)*			
Absent	81 (80.2%)	9 (81.8%)	0.898
Present	20 (19.8%)	2 (18.2%)	
Lymphatic invasion (n=110)*			
Absent	71 (71.7%)	6 (54.5%)	0.238
Present	28 (28.3%)	5 (45.5%)	
Venous invasion (n=110)*			
Absent	74 (74.7%)	6 (54.5%)	0.154
Present	25 (25.3%)	5 (45.5%)	
Clinical-follow up			
Tumor grade (n=112)*			
Low	7 (6.9%)	0 (0%)	0.367
High	94 (92.1%)	11 (100%)	

* Total number of cases lower than 113 due to missing clinical information

(Continued)

Supplementary Table VIII – Continued.

Parameters	*RAS*		p-value
	WT	Mutated	
Clinical-follow up			
Staging T (n=112)*			
Ta / Tis	7 (6.9%)	0 (0%)	
T1	26 (25.5%)	1 (9.1%)	
T2	18 (17.6%)	1 (9.1%)	0.357
T3	43 (42.2%)	8 (72.7%)	
T4	8 (7.8%)	1 (9.1%)	
Staging N (n=109)*			
N0/Nx	92 (93.9%)	9 (81.8%)	
N1	4 (4.1%)	2 (18.2%)	0.366
N2	2 (2.0%)	0 (0%)	
Staging M (n=97)*			
M0/Mx	75 (85.2%)	9 (100%)	0.215
M1	13 (14.8%)	0 (0%)	
Treatment procedure (n=114)			
Nephroureterectomy	94 (91.3%)	11 (100%)	
Partial ureterectomy	7 (6.8%)	0 (0%)	0.593
Nephroscopy with resection	2 (1.9%)	0 (0%)	
Residual tumor (n=110)*			
R0	86 (86.9%)	10 (90.9%)	
R1	9 (9.1%)	1 (9.1%)	0.793
R2	4 (4.0%)	0 (0%)	

* Total number of cases lower than 113 due to missing clinical information

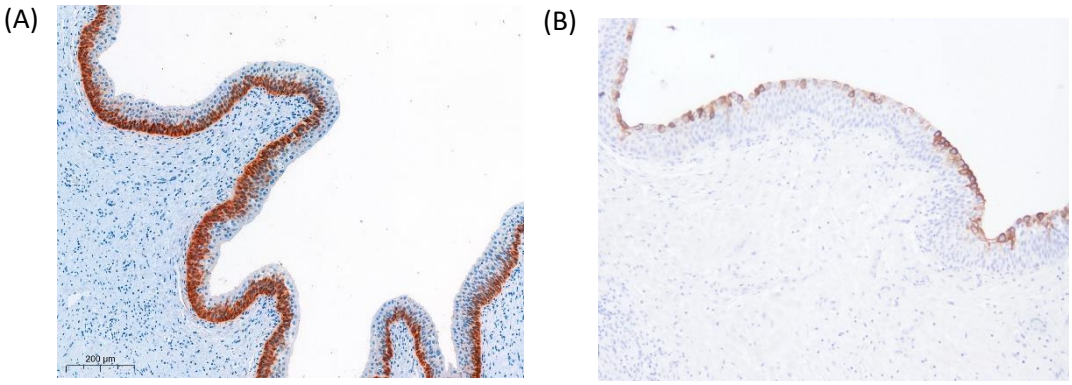

Supplementary Figure VI. Representative section of normal upper urinary tract tissue for (A) CK5/6 (scale bar of 200µm) and (B) CK20 expression patterns (100x magnification)